

NASA TMX # 55659

# A PRELIMINARY REPORT ON BIDIRECTIONAL REFLECTANCES OF STRATOCUMULUS CLOUDS MEASURED WITH AN AIRBORNE MEDIUM RESOLUTION RADIOMETER

BY

G.T. CHERRIX  
B.A. SPARKMAN

FEBRUARY 1967



**GODDARD SPACE FLIGHT CENTER**  
**GREENBELT, MARYLAND**

**N67-18660**

FACILITY FORM 602

(ACCESSION NUMBER)

38

(PAGES)

NASA-TMX-55659

(NASA CR OR TMX OR AD NUMBER)

(THRU)

1

(CODE)

20

(CATEGORY)

A PRELIMINARY REPORT ON BIDIRECTIONAL REFLECTANCES  
OF STRATOCUMULUS CLOUDS MEASURED WITH AN AIRBORNE  
MEDIUM RESOLUTION RADIOMETER

by

G. T. Cherrix  
B. A. Sparkman

February 1967

Goddard Space Flight Center,  
Greenbelt, Maryland

PRECEDING PAGE BLANK NOT FILMED.

A PRELIMINARY REPORT ON BIDIRECTIONAL  
REFLECTANCES OF STRATOCUMULUS CLOUDS  
MEASURED WITH AN AIRBORNE MEDIUM  
RESOLUTION RADIOMETER

by

G. T. Cherrix  
B. A. Sparkman

ABSTRACT

Bidirectional reflectances of three stratocumulus clouds were measured with the two visible channels, (0.55 to 0.85 $\mu$ , and .2 to 4 $\mu$ ), of an airborne Medium Resolution (Infrared) Radiometer. These measurements were made in five azimuth directions with respect to the principal plane of the sun. Values of bidirectional reflectances obtained agree well with those expected from Mie scattering theory. The albedo of each stratocumulus cloud was derived by summing bidirectional reflectances over a hemisphere.

PRECEDING PAGE BLANK NOT FILMED.

CONTENTS

	<u>Page</u>
ABSTRACT.....	iii
INTRODUCTION .....	1
INSTRUMENTATION .....	2
METHOD OF MEASUREMENT .....	3
ALBEDO CALCULATIONS .....	3
RESULTS AND CONCLUSIONS .....	5
ACKNOWLEDGEMENTS .....	6
REFERENCES .....	6

A PRELIMINARY REPORT ON BIDIRECTIONAL REFLECTANCES  
OF STRATOCUMULUS CLOUDS MEASURED WITH AN AIRBORNE  
MEDIUM RESOLUTION RADIOMETER

by

G. T. Cherrix  
B. A. Sparkman

INTRODUCTION

Albedos of clouds have been measured since the early 1900's from balloons<sup>1</sup>, blimps<sup>2</sup>, aircraft<sup>3,4,5</sup>, and now from satellites<sup>6,7</sup>. Most of these measurements have been made with wide field of view ( $2\pi$  steradian) sensors. Since the advent of meteorological satellites like Tiros and Nimbus, earth albedos have been determined from narrow field of view satellite sensors. A satisfactory method of summing these measurements to obtain albedo values has not yet been found. Reflected radiation from clouds is anisotropic and is greatly dependent on the solar zenith angle. Measurements by Coulson<sup>8</sup>, Blau<sup>9</sup>, Bartman<sup>10</sup>, and others show this effect. For large zenith angles it is strongly anisotropic with most of the energy scattered in the forward direction. For small zenith angles the radiation is reflected nearly isotropically. The magnitude of this anisotropy, its zenith angle dependence, and its effect on the total albedo of a cloud are not well known.

Measurements of bidirectional reflectances of several clouds with various solar zenith angles were made in the spring of 1966 and will be continued in the spring of 1967 to add more information to help answer this question. Data from three selected rosettes flown over stratocumulus clouds are used in this preliminary investigation.

## INSTRUMENTATION

### Medium Resolution Infrared Radiometer

The instrument used to measure bidirectional reflectances is the Nimbus type, 5 channel Medium Resolution Infrared Radiometer, (MRIR). Three of the channels, (see Fig. 1) respond to the infrared region of the spectrum. (Channel 1,  $6.7\mu$ , channel 2, 10 to  $11\mu$ , and channel 4, 5 to  $30\mu$ ). Channels 3 ( $0.55$  to  $0.85\mu$ ) and 5 ( $0.2$  to  $4\mu$ ) respond to the short wave region. This report is concerned solely with measurements in the short wave region.\*

Figure 2 shows the MRIR without modifications for mounting on the aircraft. Figure 3 is a diagram of the optical system of each channel. Only the filter (F) is different for these two channels. The scan mirror (M) rotates about an axis parallel to the axes of the 5 casagrainian telescopes such that each 50 by 50 milliradian field of view scans through a  $360^\circ$  arc in a plane perpendicular to the axis of rotation in  $7\text{-}1/2$  seconds. The airborne instrument scans in the vertical plane containing the longitudinal axis of the aircraft. The instrument was covered with a thick thermal foam jacket without obscuring the field of view and scanning area. Heaters were provided to maintain the radiometer at  $25^\circ\text{C}$ . This assembly was shock mounted inside an aerodynamic fairing which was fastened to the underside of the tail section of NASA's Convair 990 jet aircraft. Figure 4 shows the MRIR mounted in the aerodynamic fairing. A motor operated door was provided in the fairing to protect the optics of the MRIR during take-off and landing. Figure 5 shows the unobscured field of view of the short-wave channels of the MRIR. Scanning was fore-to-aft in the downward looking direction.

### Sol-A-Meters

The Sol-A-Meters are silicon (photo-voltaic) solar cells. Two Sol-A-Meters were carried, one mounted on the downward facing surface of the MRIR aerodynamic fairing, (see Fig. 4), and one mounted behind the aircraft vertical stabilizer on an upward facing platform. The cells are calibrated to indicate insolation over a full  $2\pi$  steradian field of view within the spectral range from  $0.35$  to  $1.15$  microns. Figure 6 gives the spectral response curve of a silicon

---

\*The term "Medium Resolution Infra-red Radiometer" (MRIR) is actually a misnomer, since the satellite instrument contains a channel which responds in part to visible radiation ( $.2\mu$  to  $4\mu$ ), and the airborne instrument contains two such channels ( $0.55\mu$  to  $0.85\mu$ , and  $0.2\mu$  to  $4\mu$ ). However, the term "MRIR" has been so widely adopted as to compel its use here.

solar cell. The ratio of the signal from the downward looking cell to that of the upward looking cell is used to calculate albedo.

## METHOD OF MEASUREMENT

To measure bidirectional reflectances to obtain albedo with the airborne MRIR, it is desirable to take measurements in as many nadir and azimuthal direction as possible. Because of the length of time required to maneuver the Convair 990 aircraft, and since solar zenith angle and cloud patterns are constantly changing, it is necessary to measure the bidirectional reflectance of a cloud in as short a time as possible. Therefore, a rosette flight pattern, as shown in Fig. 7, was chosen. With this flight path, bidirectional reflectances with nadir angles ( $0 \leq \theta < 90^\circ$ ) are measured in 5 azimuthal directions. By assuming symmetry around the principal plane of the sun (directions 1 and 2 in Fig. 7), bidirectional reflectances are obtained for 8 directions. These reflectance measurements are then integrated over a hemisphere by the method shown in the following section to obtain albedos. Figure 8 shows the method of designating angles used in the albedo calculations.

## ALBEDO CALCULATIONS

The energy reflected from a surface over a hemisphere is:

$$\bar{W} = \bar{H}^* \cos \zeta_0 \int_{\phi=0}^{2\pi} \int_{\theta=0}^{\pi/2} \rho(\theta\phi) \cos \theta \sin \theta \, d\theta d\phi \quad (1)$$

where  $\bar{H}^* \cos \zeta_0$  is the effective solar irradiance and  $\zeta_0$  is the solar zenith angle.  $\bar{H}^*$  is obtained by integrating the spectral solar irradiance,  $\bar{H}_\lambda^*$  as given by Johnson<sup>11</sup>, and the effective spectral response function  $\phi_\lambda$  of each channel over all wave lengths.

$$\bar{H}^* = \int_0^\infty \bar{H}_\lambda^* \phi_\lambda \, d\lambda \quad (2)$$

The bidirectional reflectance,  $\rho(\theta\phi)$  is a function of azimuth and nadir angle.

$$\rho(\theta\phi) = \frac{\bar{N}(\theta\phi)}{\bar{H}^* \cos \zeta_0} \quad (3)$$

where  $\bar{N}$  is the measured effective radiance.

Albedo, by definition, is the ratio of the amount of radiation reflected by a body to the amount incident upon it. Therefore Albedo, A, is:

$$A = \frac{\bar{W}}{\bar{H}^* \cos \zeta_0} \quad (4)$$

Thus the albedo of a cloud in terms of bidirectional reflectance is:

$$A = \frac{\bar{W}}{\bar{H}^* \cos \zeta_0} = \int_{\phi=0}^{2\pi} \int_{\theta=0}^{\pi/2} \rho(\theta\phi) \cos \theta \sin \theta \, d\theta d\phi \quad (5)$$

In using aircraft data Eq. (5) is approximated numerically by the summation:

$$A = \sum_{j=1}^8 \sum_{i=2}^{18} \rho(\theta\phi) \cos \theta \sin \theta \, [\Delta\theta]_i \, [\Delta\phi]_j \quad (6)$$

In order to sum the reflectance measurements, one must also assume symmetry for  $22\text{-}1/2^\circ$  on each side of the 8 azimuthal directions. The cloud surface is thereby divided into 8 -  $45^\circ$  sections, each having one value of bidirectional reflectance for nadir angles  $0^\circ$  to  $90^\circ$ . Therefore  $\Delta\phi = \pi/4$ . Summing is done over  $5^\circ$  nadir angle intervals so that  $\Delta\theta = \pi/36$ . Thus, the bidirectional reflectance is summed over each octant, then the octant values are summed for albedo.

## RESULTS AND CONCLUSIONS

Table 1 shows albedos for channel 3 and 5 for each of the clouds. These values of cloud albedos agree with those of Luckeish<sup>3</sup>, who measured 0.36 for thin clouds to 0.78 for dense clouds. Measurements by Blau<sup>12</sup>, Aldrich<sup>1</sup>, Neiburger<sup>2</sup>, and others also fall in this range. This wide range exists because albedos of clouds vary with the thickness, structure, and altitude of the cloud, and the reflectivity of the underlying surface.

Table I

Target	Solar Zenith Angle		% Albedo		% Albedo
	Begin Rosette	End Rosette	0.55 to 0.85 $\mu$	0.2 to 4 $\mu$	Sol-A-Meters
Stratocumulus Over Pacific Ocean	75°25'	68°50'	40.3	31.9	41.9
Stratocumulus Over Pacific Ocean	74°15'	66°41'	52.0	43.1	55.8
Stratocumulus Over Okeefenokee	73°10'	73°10'	70.6	57.6	70.8

The cloud albedos measured by channel 3 are always higher than those of channel 5, presumably because of the water vapor and carbon dioxide absorption in the long wave length portions of channel 5's sensitivity range.

Albedos indicated by the Sol-A-Meters are also listed in Table 1 and agree well with the MRIR values.

Figures 9 through 26 show the bidirectional reflectances with nadir angle for each azimuthal direction flown. All of these cases have large solar zenith angles and a strong component of forward scattering in the principal plane of the sun, as expected from Mie scattering theory. Bidirectional reflectances of similar magnitudes were also measured by Coulson<sup>8</sup>, Blau<sup>9</sup>, and Bartman<sup>10</sup>.

This large component of bidirectional reflectance at low sun angles shows that anisotropic backscatter should be accounted for when satellite beam measurements of reflectances at low sun angles are used to calculate albedos.

## ACKNOWLEDGEMENTS

We would like to thank Mr. William Bandeen for his guidance in this work. We would also like to thank Mr. William Fizell who did most of the calculations on which this paper is based.

## REFERENCES

1. Aldrich, L. B., "The Reflecting Power of Clouds," Smithsonian Misc. Coll., 69, No. 10, (1919).
2. Neiburger, M., "Reflection, Absorption and Transmission of Insolation by Stratus Clouds," J. Meteor., Vol. 6, pp. 98-104, (1919).
3. Luckiesh, M., "Aerial Photometry," Astrophys. Jour., Vol. 49, pp. 108-130, (1919).
4. Bauer, K. G., and J. A. Dutton., "Albedo Variations Measured from An Airplane over Several Types of Surface," J. Geophys. Res. 67(6), 2367-2376, 1962.
5. Marlatt, W. E., "Investigations of the Temperature and Spectral Emissivity Characteristics of Cloud Tops and of the Earth Surface," Report NASA Contr. No. NASr-147, Feb. 1964.
6. Bandeen, W. R., Halev, M. and Strange, I., "A Radiation Climatology in the Visible and Infrared From the TIROS Meteorological Satellites," NASA TND-2534, National Aeronautics and Space Administration, Washington, D.C., June 1965.
7. House, F. B., "The Radiation Balance of the Earth From a Satellite," Ph.D. Dissertation, Univ. of Wisconsin, Dept. of Meteorology, 1965.
8. Coulson, K. K., G. M. Bouricius and E. L. Gray, "Effects of Surface Reflection on Radiation Emerging From the Top of a Planetary Atmosphere," Report NASA Contr. No. NAS5-3925, Sept. 1965.
9. Blau, Henry H., Jr., Ronald P. Espinola, and Edward C. Rufenstein, III, "Near Infrared Scattering by Sunlit Terrestrial Clouds," Appl. Opt. 5, 555, (1966).
10. Bartman, F. L., "The Reflectance and Scattering of Solar Radiation by the Earth." Preliminary Report NASA Contr. NASr-54(03), Feb. 1967.

11. Johnston, F. S. Ed., "Satellite Environment Handbook" (Stanford University Press, Stanford, Calif., 1961).

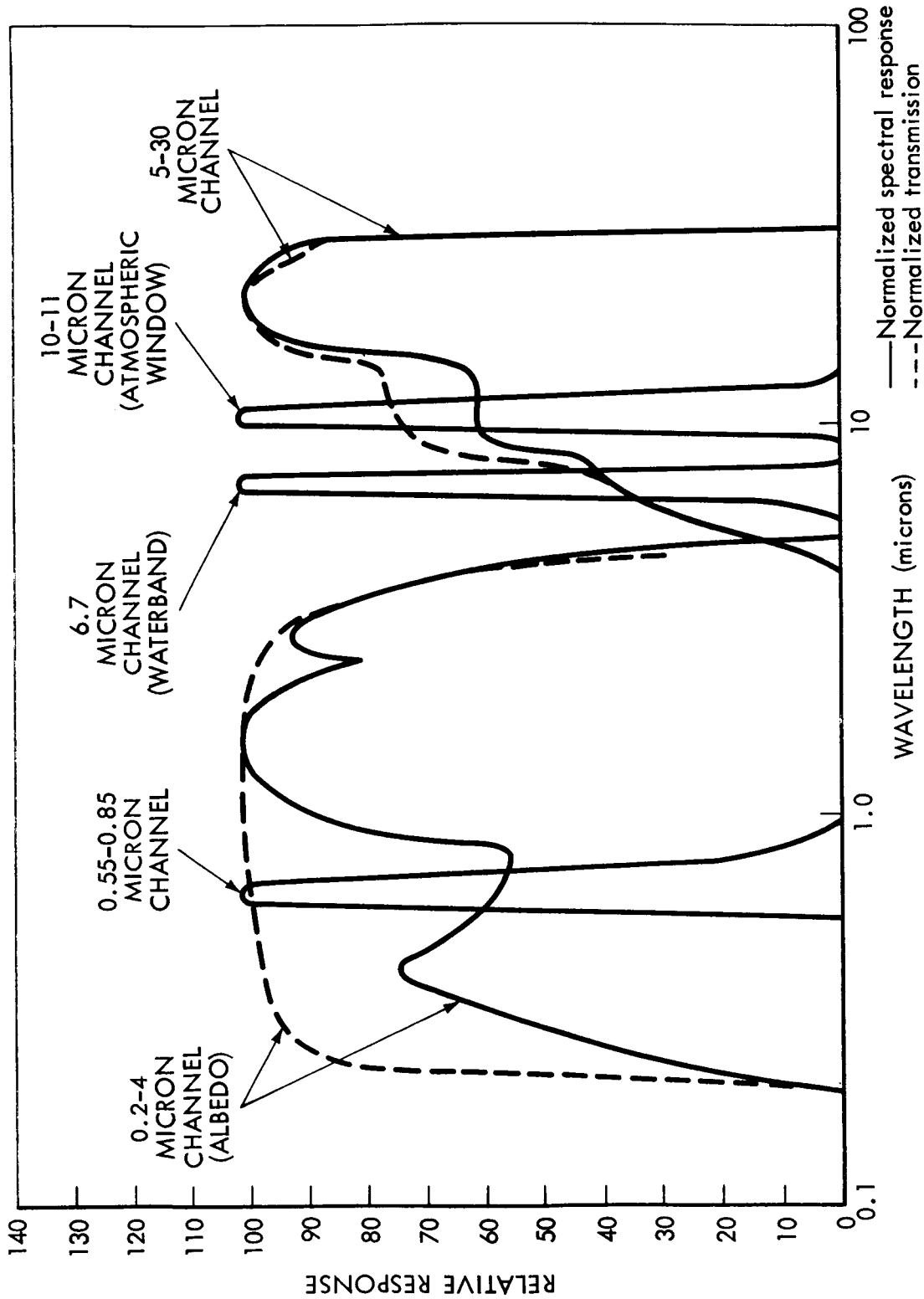


Figure 1—Filter and Relative Spectral Response of Nimbus Five-Channel Radiometer

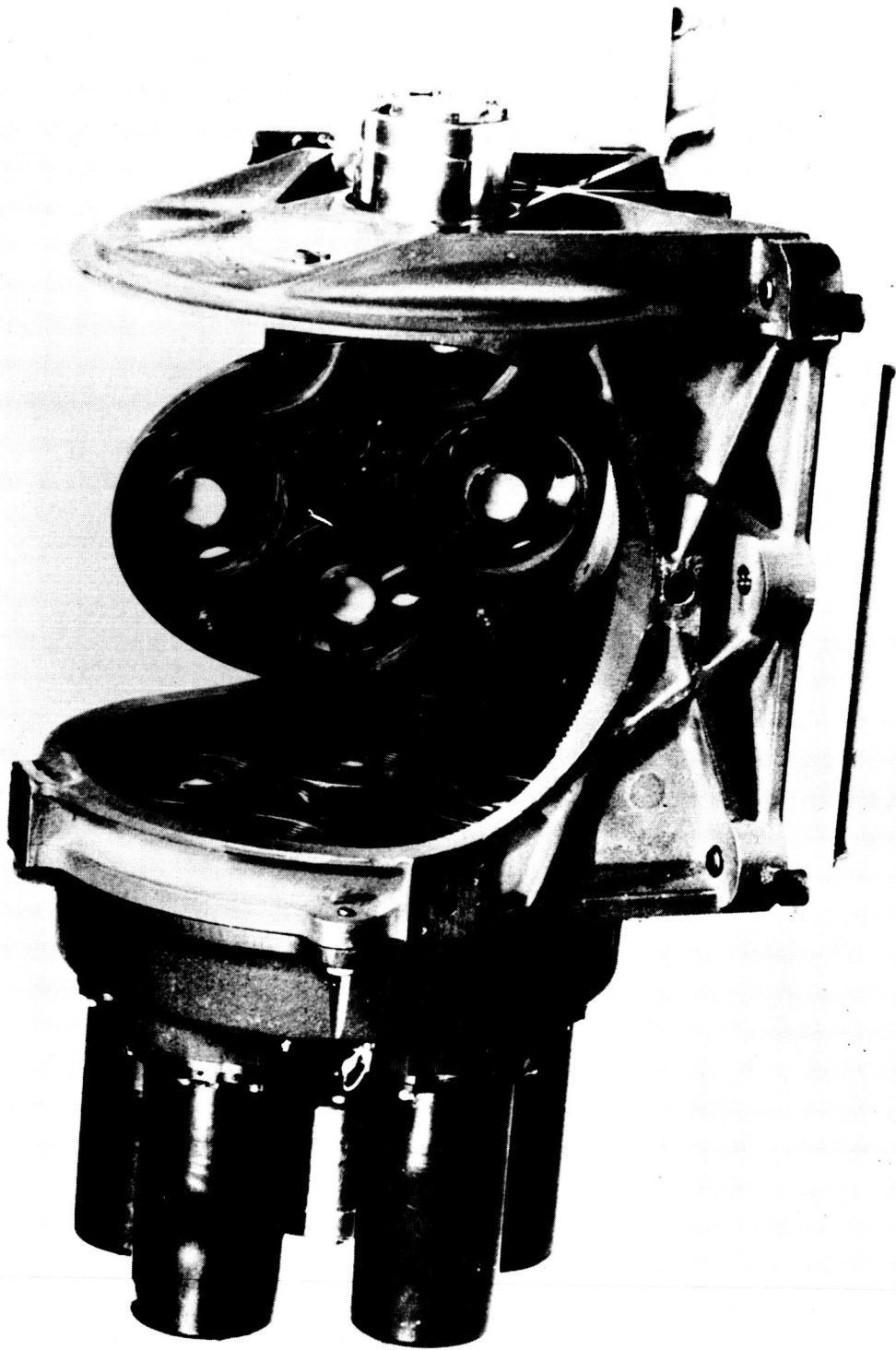
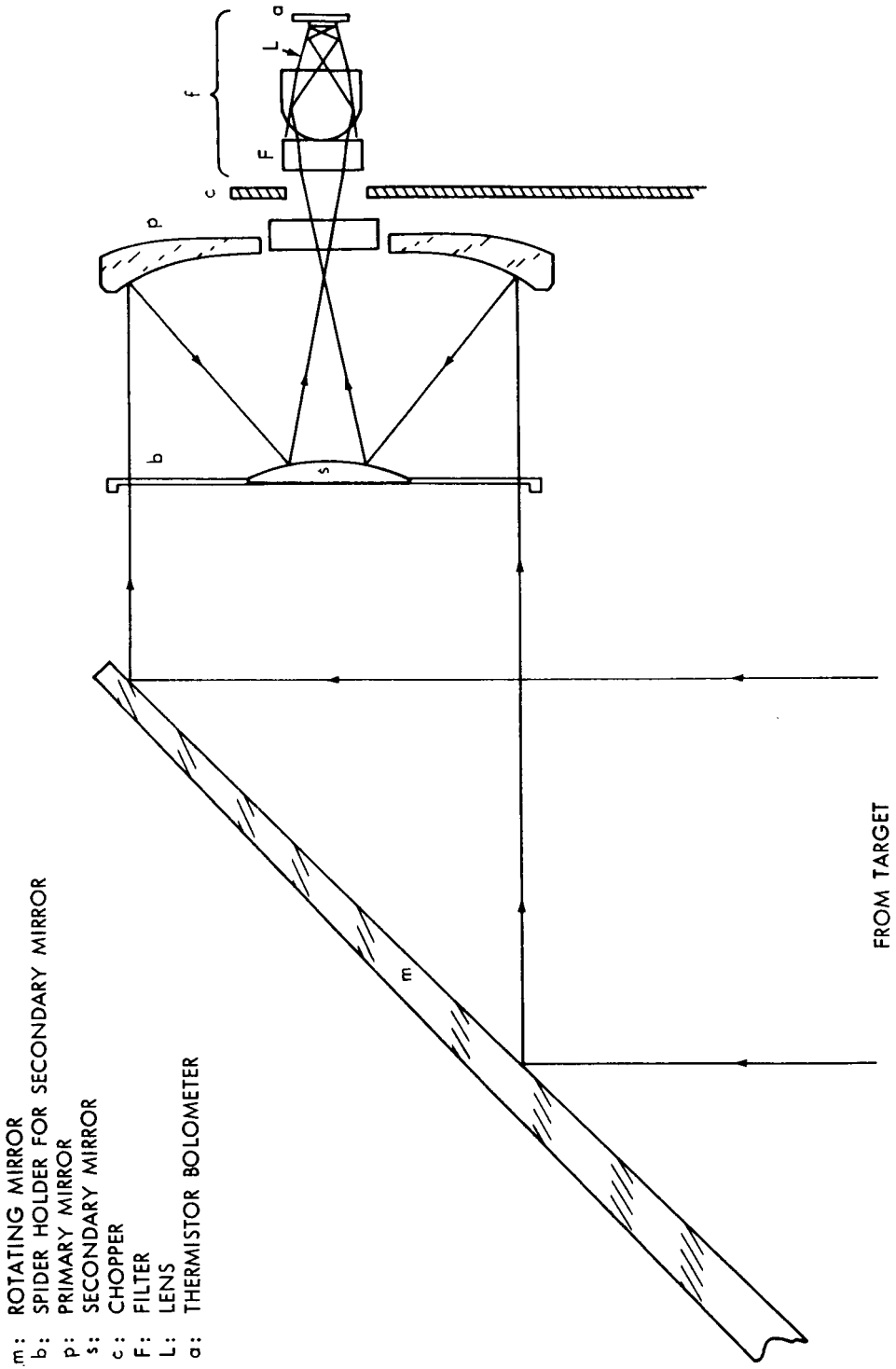


Figure 2—Medium Resolution Infrared Radiometer, (MRIR)



- m: ROTATING MIRROR
- b: SPIDER HOLDER FOR SECONDARY MIRROR
- p: PRIMARY MIRROR
- s: SECONDARY MIRROR
- c: CHOPPER
- F: FILTER
- L: LENS
- a: THERMISTOR BOLOMETER

FROM TARGET

Figure 3—Optical System of the MRIR

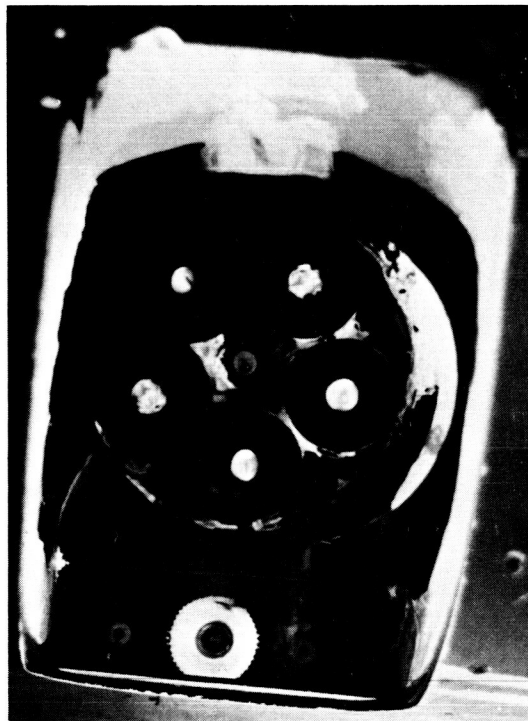
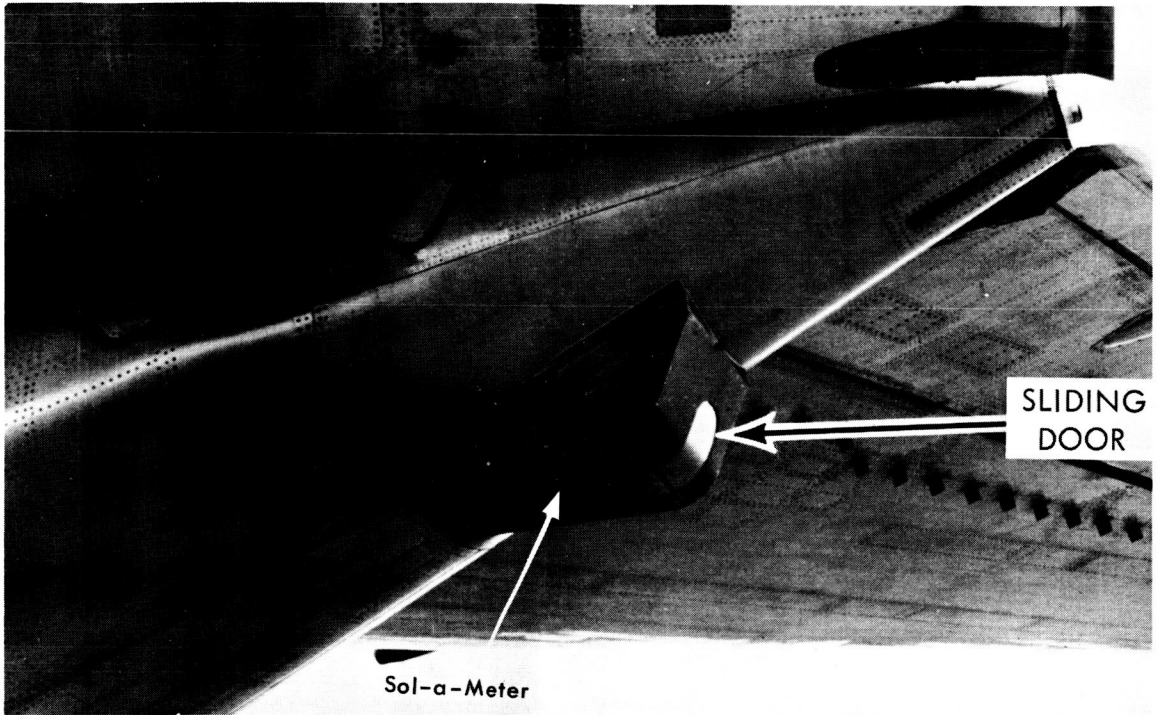


Figure 4—MRIR and Sol-A-Meter Mounted in Aircraft Fairing

EARTH-SKY PORTION OF FIELD OF VIEW OF  
ALBEDO CHANNELS OF MRIR MOUNTED  
ON JET AIRCRAFT

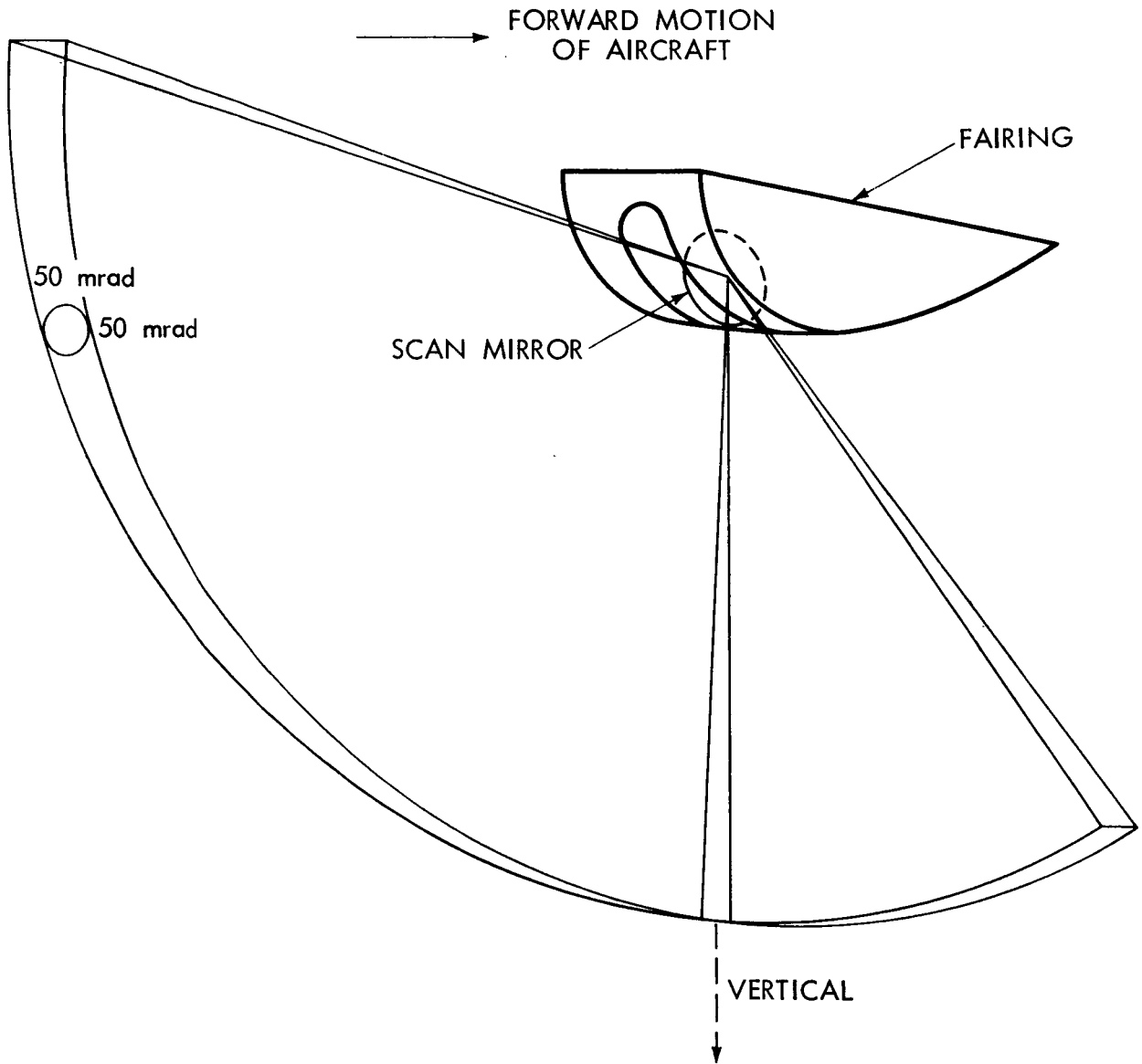
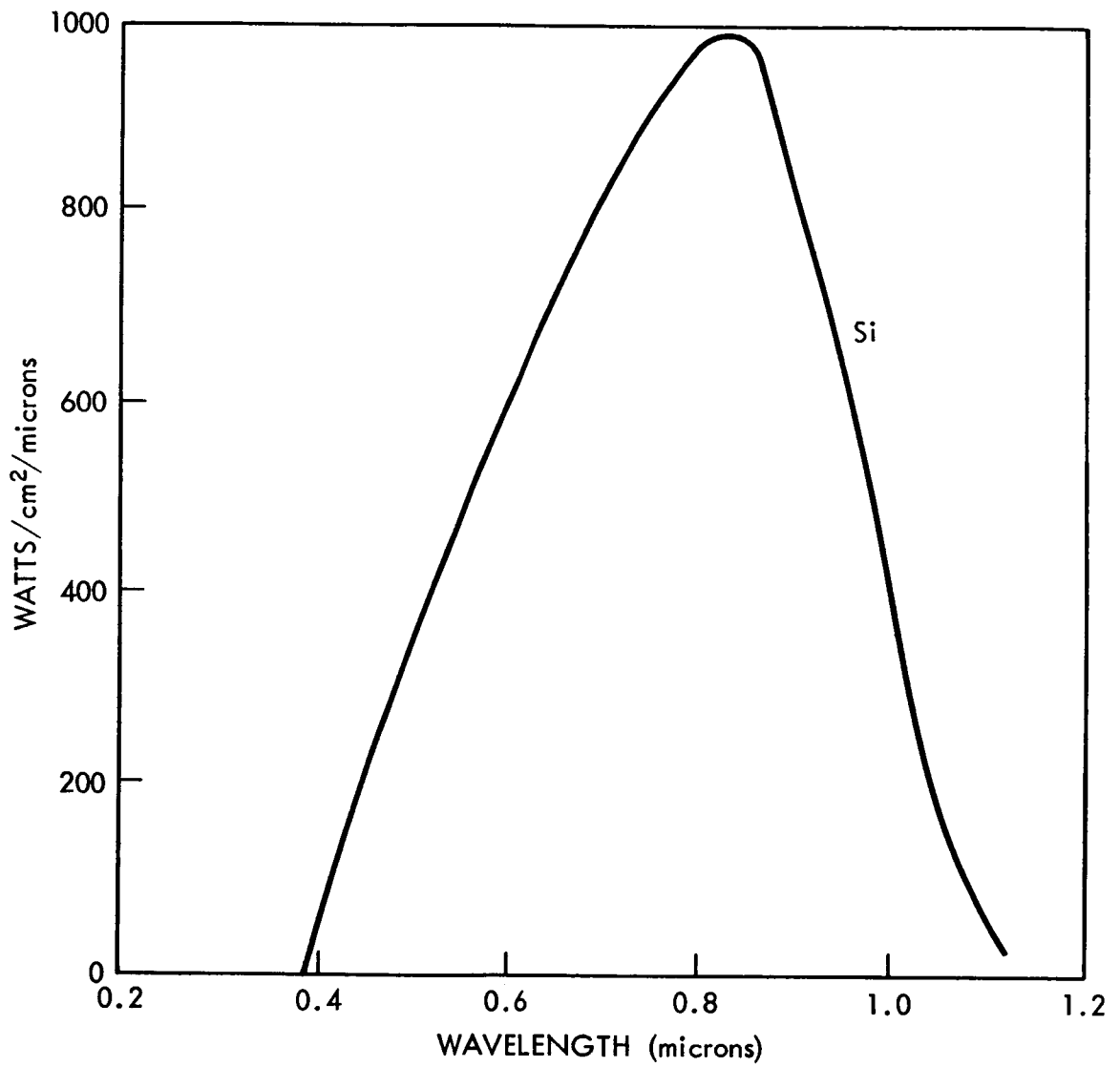


Figure 5—Earth-Sky Portion of View of Albedo Channels of MRIR Mounted on Jet Aircraft



SILICON CELL SPECTRAL RESPONSE

Figure 6-Spectral Response of a Silicon Solar Cell

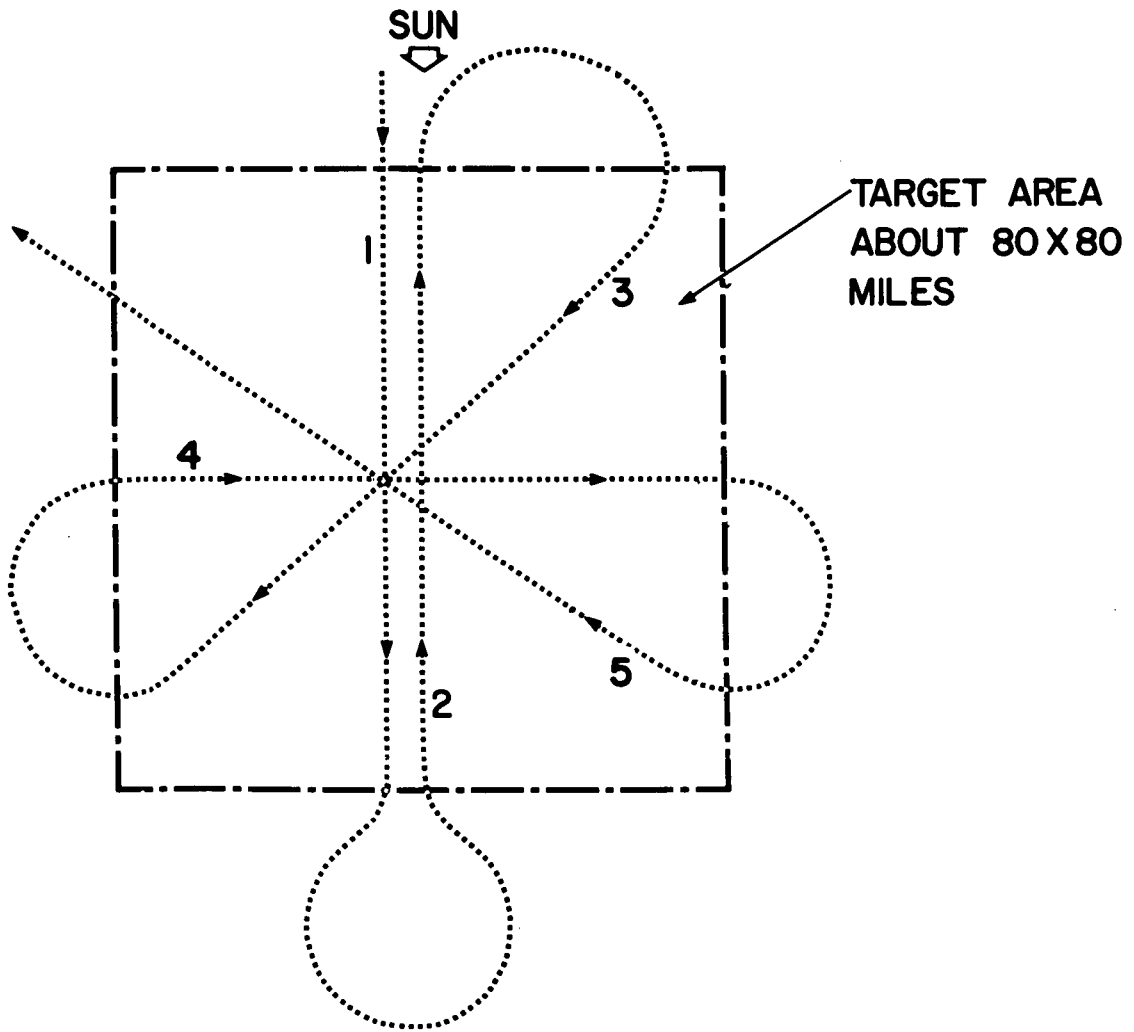
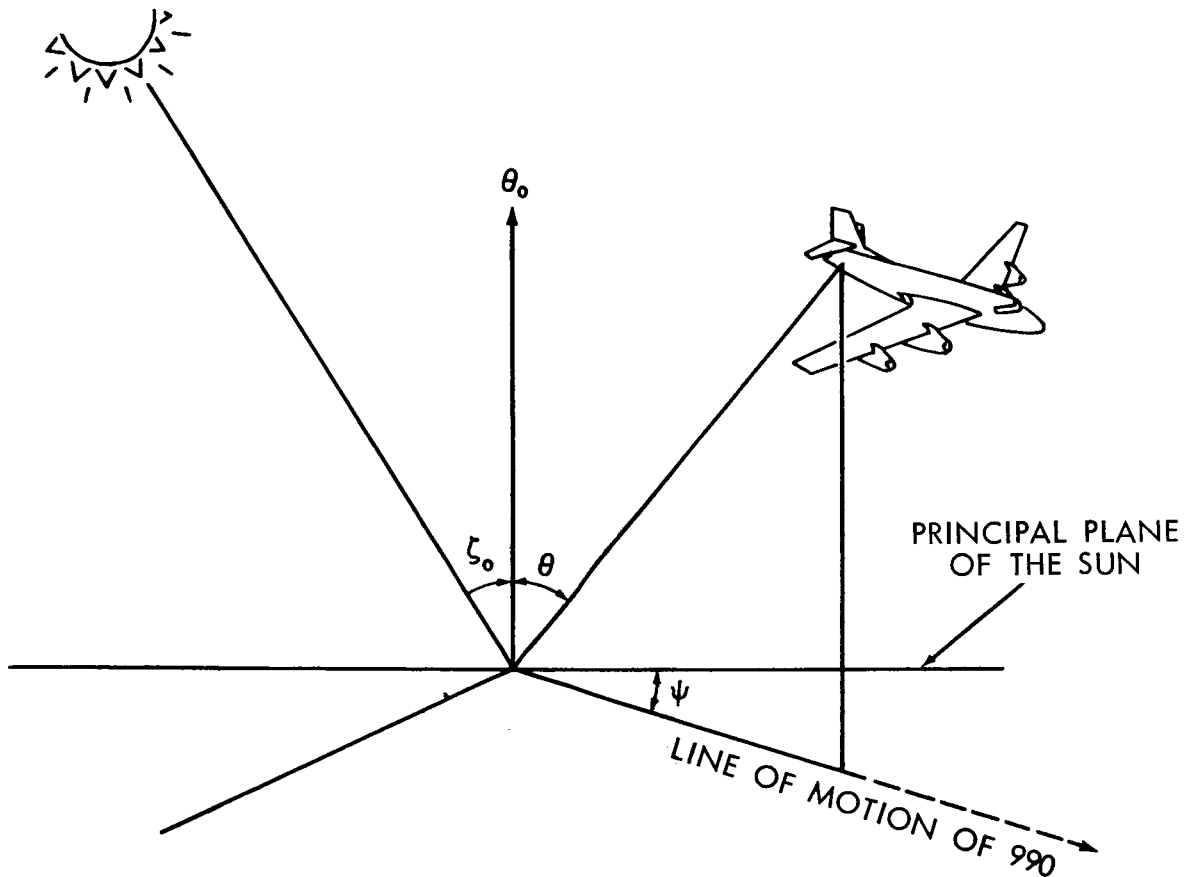


Figure 7-Rosette Flight Pattern



$\zeta_0$  = SOLAR ZENITH ANGLE

$\theta$  = NADIR ANGLE OF REFLECTED ENERGY

$\psi$  = HORIZONTAL ANGULAR DEPARTURE OF 990'S FLIGHT PATH OUT OF THE PRINCIPAL PLANE OF THE SUN

$\theta_0$  = LOCAL VERTICAL

Figure 8—Diagram Showing Solar Zenith, Azimuth, and Nadir Angles

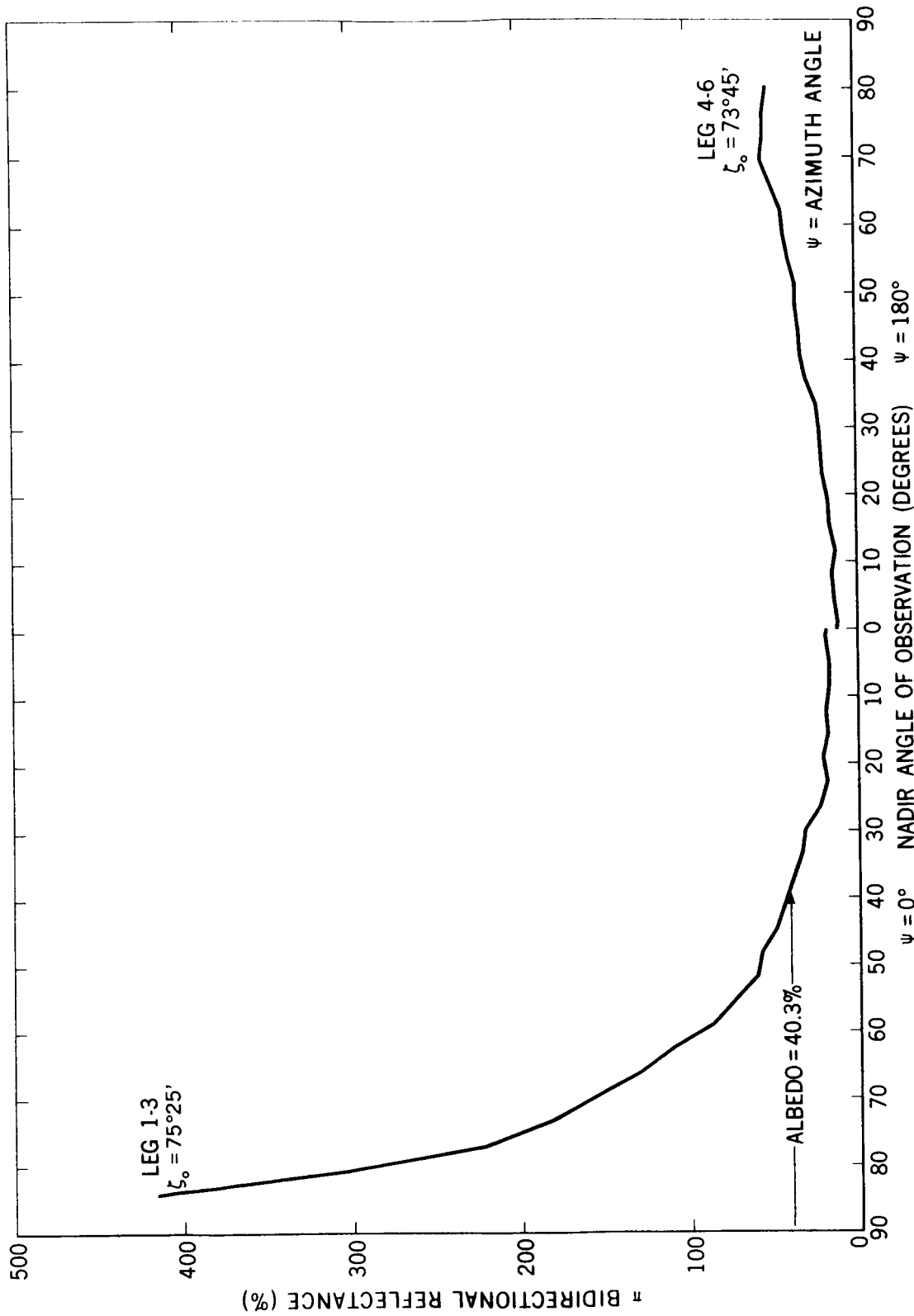


Figure 9-NASA Convair-990 Flight 37, June 15, 1966 Solid Stratocumulus (Aircraft 40,000 Ft.) 38.5° N., 129° W. (14:38 U.T. to 15:13 U.T.) MRIR Channel 3 (0.55 to 0.85 $\mu$ )

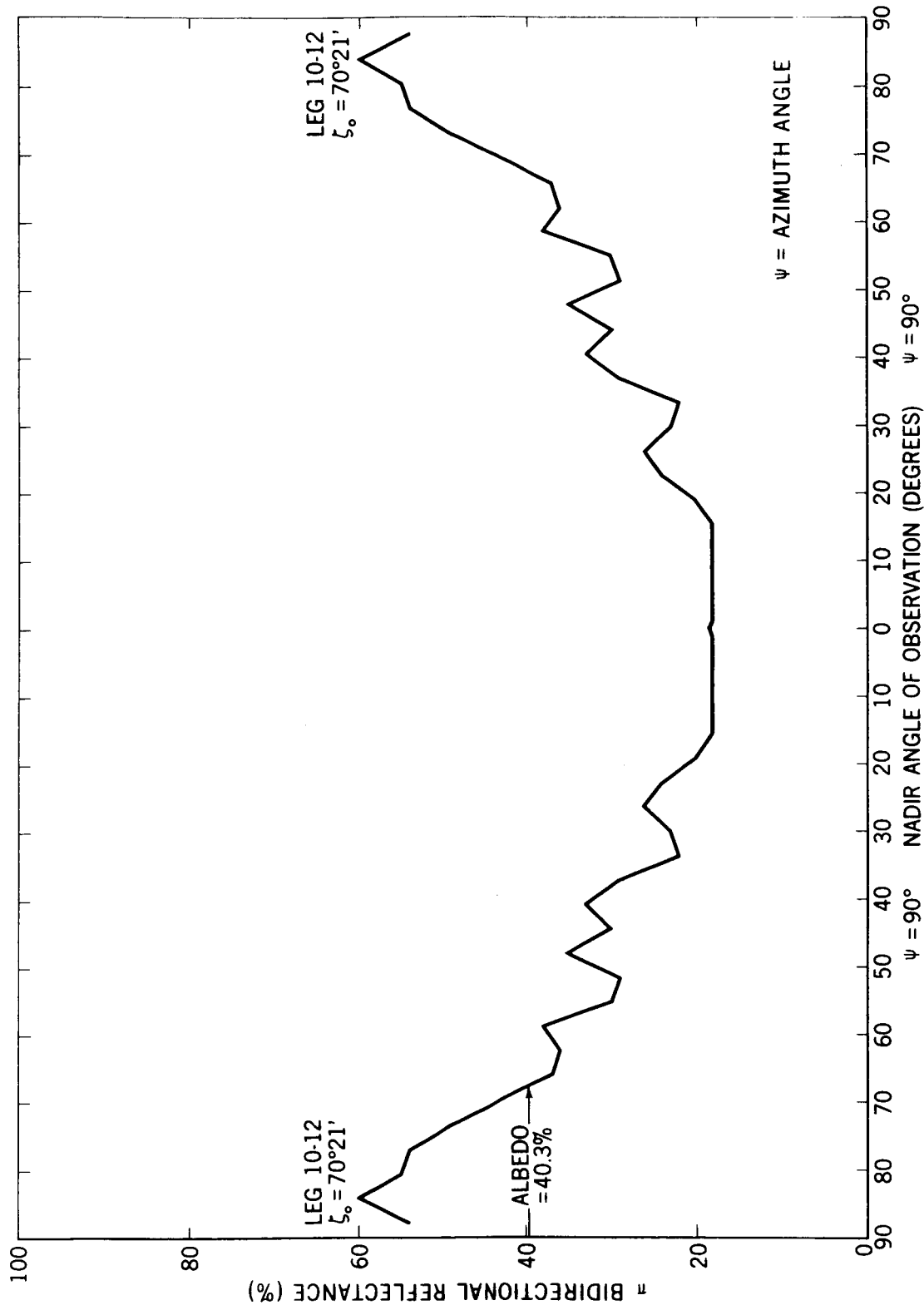


Figure 10—NASA Convair-990 Flight 37, June 15, 1966 Solid Stratocumulus (Aircraft 40,000 Ft.) 38.5° N., 129° W. (14:38 U.T. to 15:13 U.T.) MRIR Channel 3 (0.55 to 0.85 $\mu$ .)

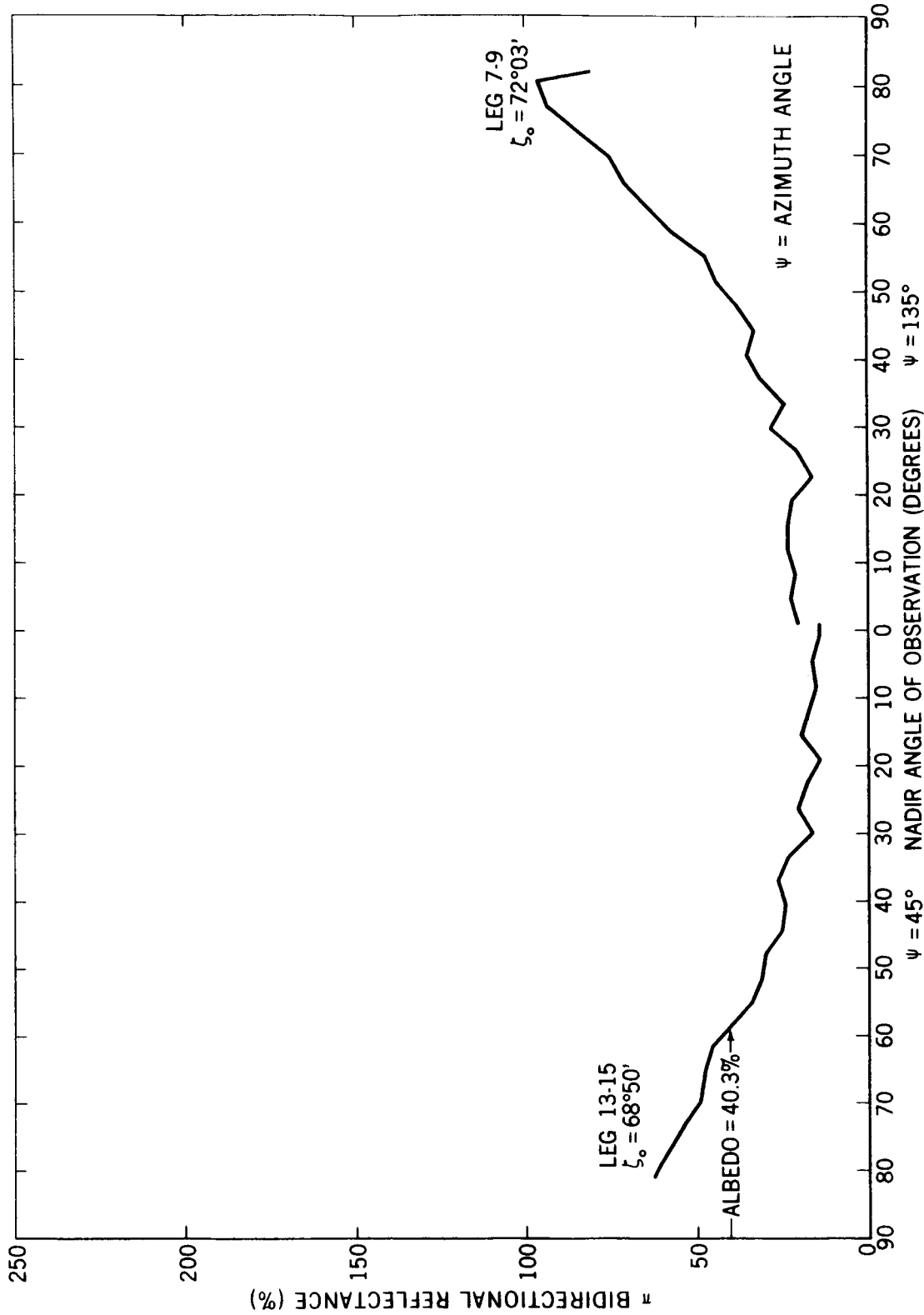


Figure 11—NASA Convair-990 Flight 37, June 15, 1966 Solid Stratocumulus (Aircraft 40,000 Ft.)  $38.5^\circ \text{N.}$ ,  $129^\circ \text{W.}$   
 (14:38 U.T. to 15:13 U.T.) MRIR Channel 3 (0.55 to  $0.85\mu$ )

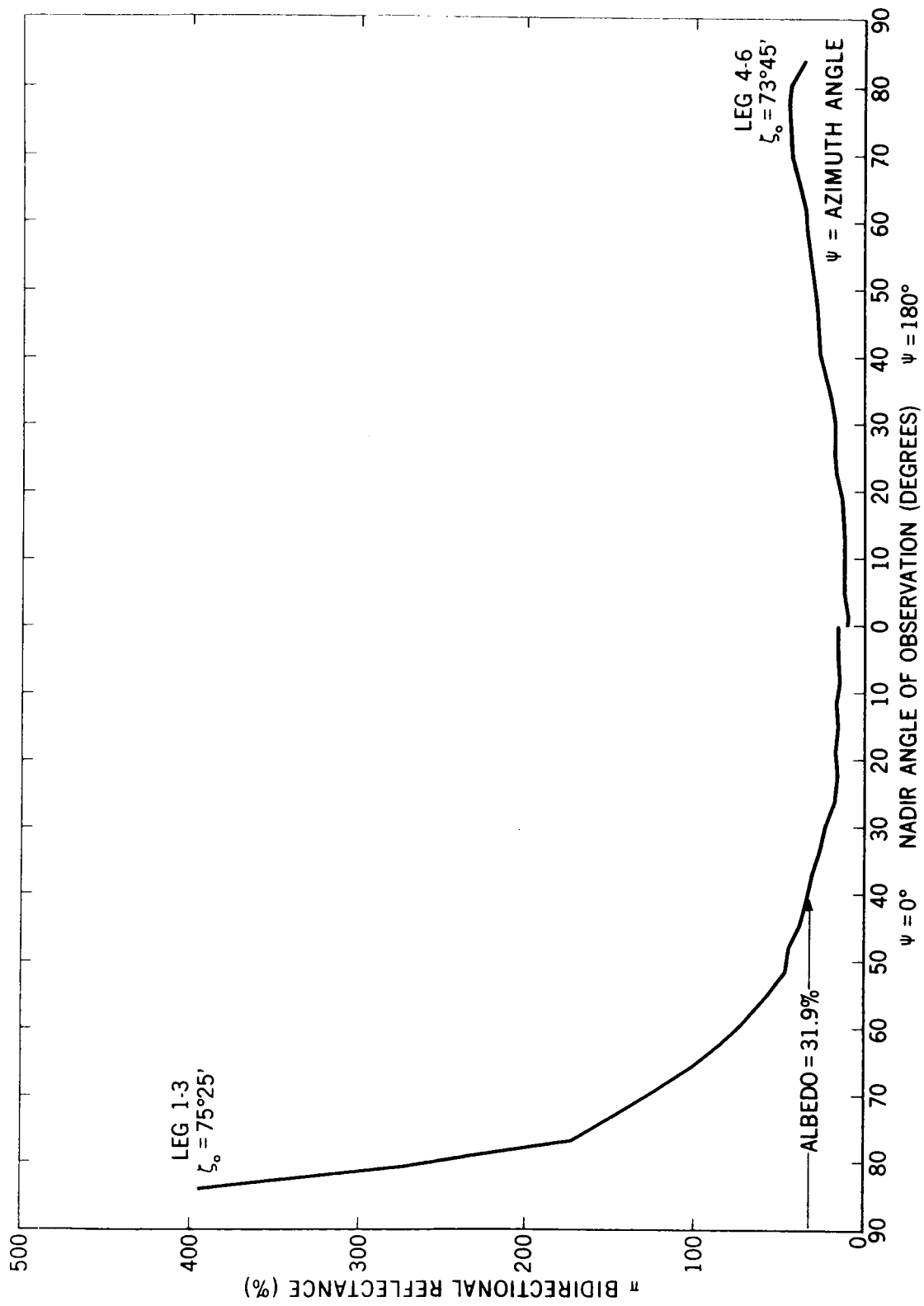


Figure 12--NASA Convair-990 Flight 37, June 15, 1966 Solid Stratocumulus (Aircraft 40,000 Ft.) 38.5° N., 129° W. (14:38 U.T. to 15:13 U.T.) MRIR Channel 5 (0.2 to 4 $\mu$ )

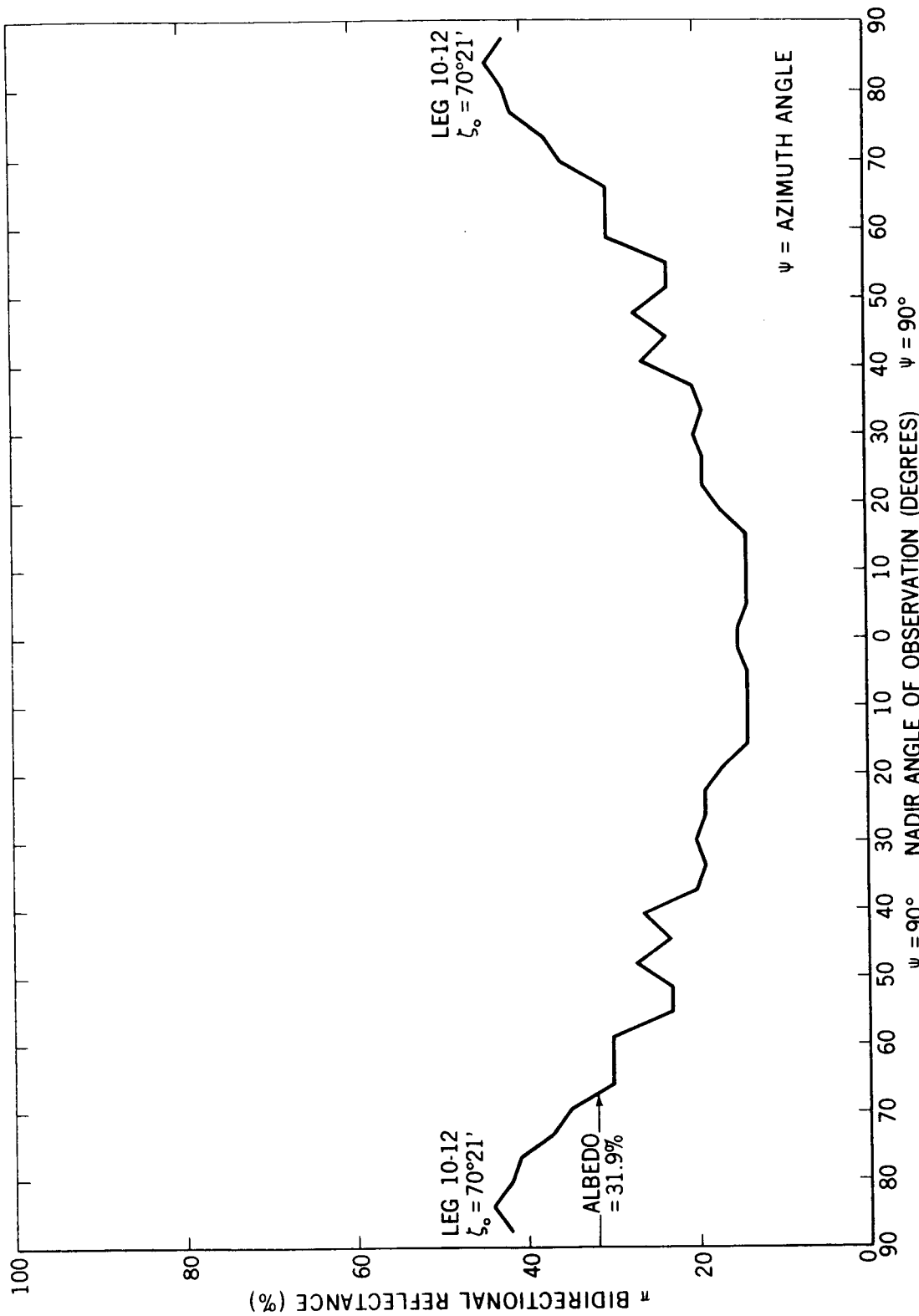


Figure 13—NASA Convair-990 Flight 37, June 15, 1966 Solid Stratocumulus (Aircraft 40,000 Ft.)  $38.5^\circ$  N.,  $129^\circ$  W. (14:38 U.T. to 15:13 U.T.) MRIR Channel 5 (0.2 to  $4\mu$ )

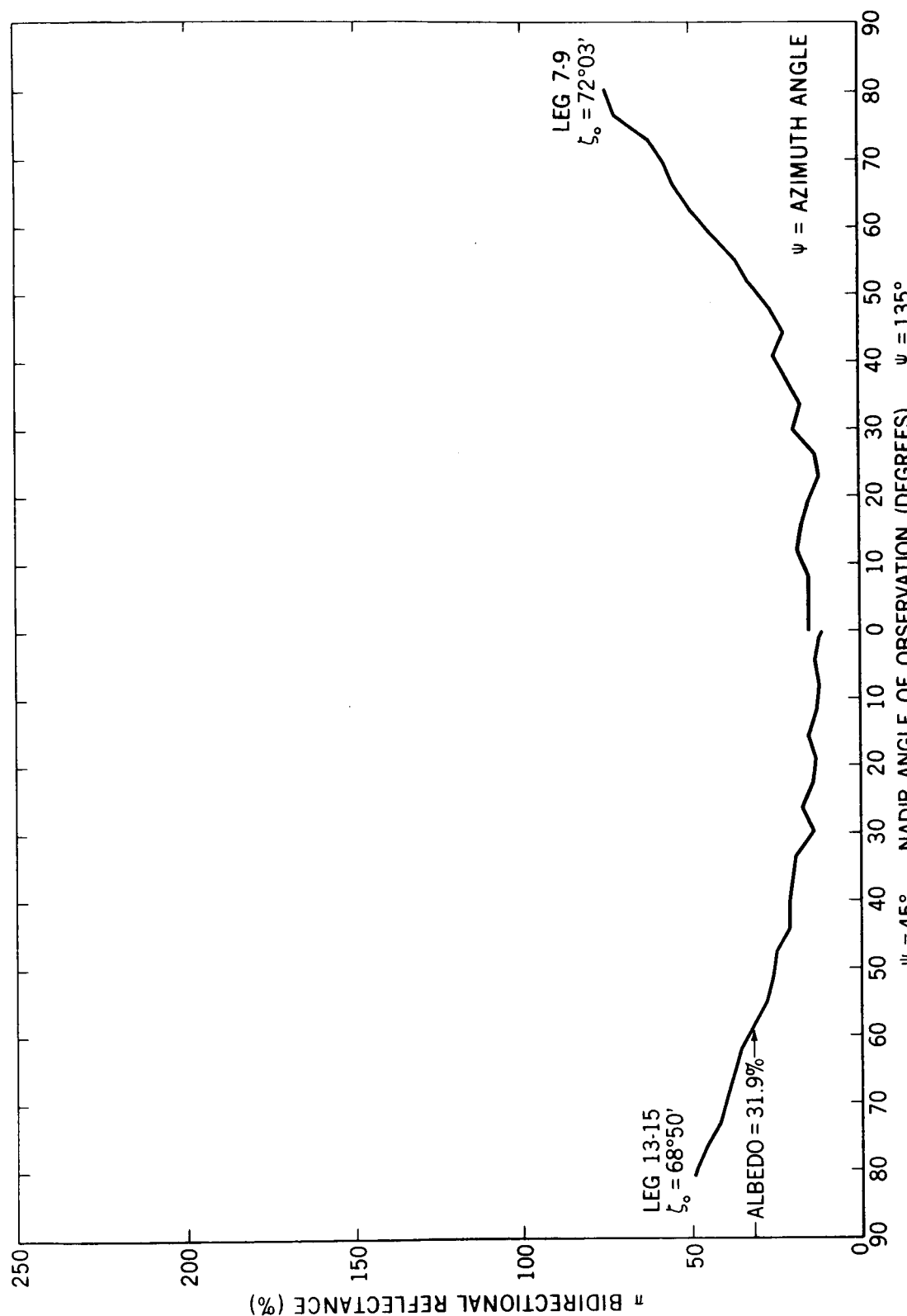


Figure 14--NASA Convair-990 Flight 37, June 15, 1966 Solid Stratocumulus (Aircraft 40,000 Ft.) 38.5° N., 129° W. (14:38 U.T. to 15:13 U.T.) MRIR Channel 5 (0.2 to 4μ)

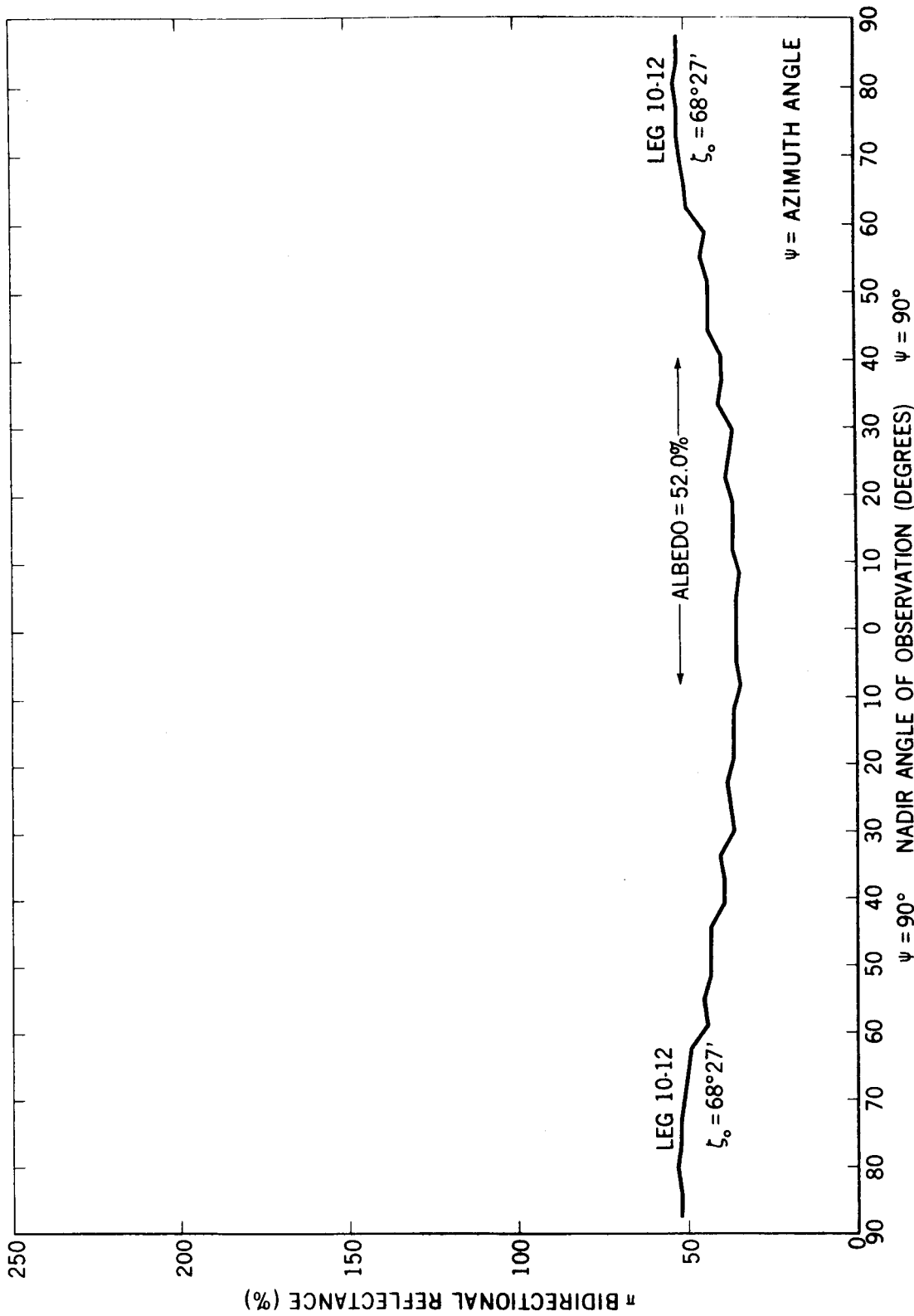


Figure 15-NASA Convair-990 Flight 36, June 14, 1966 (Alt. 40,000 Ft.) Overcast Stratocumulus (Alt. ~2,500 Ft.)  
 36.5°N., 125.0°W. (0111 U.T. to 0209 U.T.) MRIR Channel 3 (0.55 to 0.85 $\mu$ )

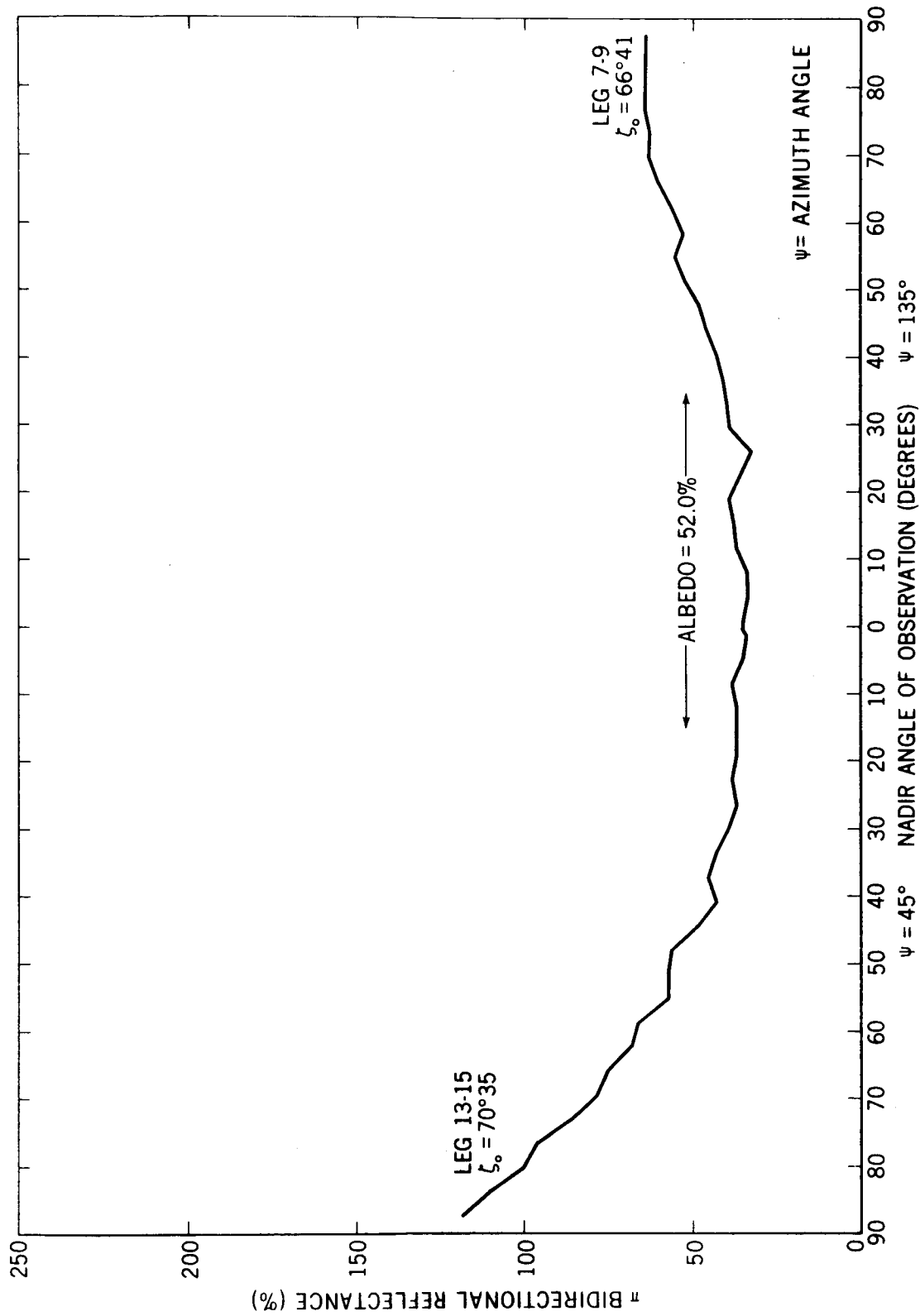


Figure 16—NASA Convair-990 Flight 36, June 14, 1966 (Alt. 40,000 Ft.) Overcast Stratocumulus (Alt. ~2,500 Ft.)  
 36.5° N., 125.0° W. (0111U.T. to 0209 U.T.) MRIR Channel 3 (0.55 to 0.85 $\mu$ )

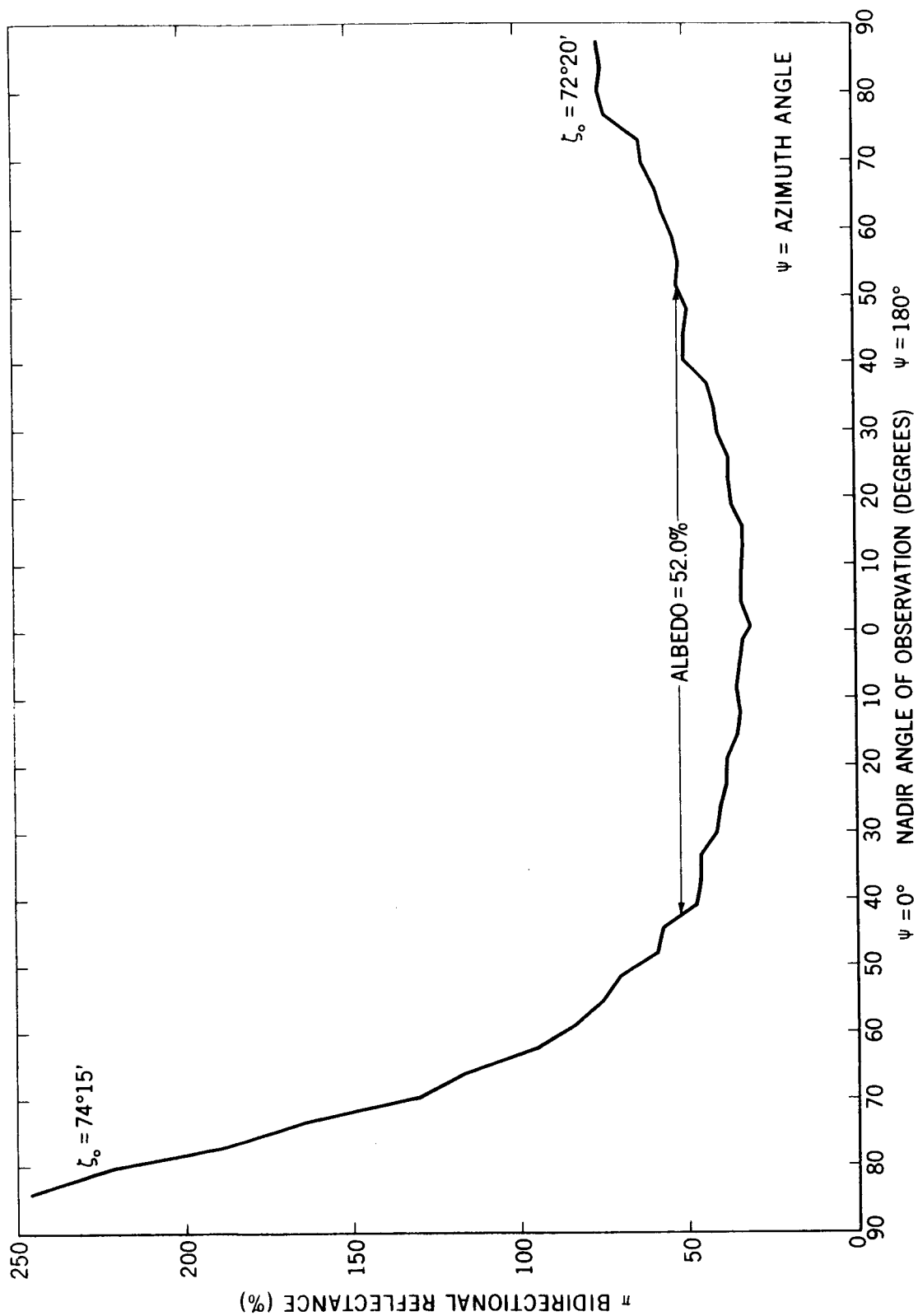


Figure 17—NASA Convair-990 Flight 36, June 15, 1966 (Alt. 40,000 Ft.) Overcast Stratocumulus (Alt. ~2,500 Ft.) 36.5° N., 125.0° W. (0111 U.T. to 0209 U.T.) MRIR Channel 3 (0.55 to 0.85μ)

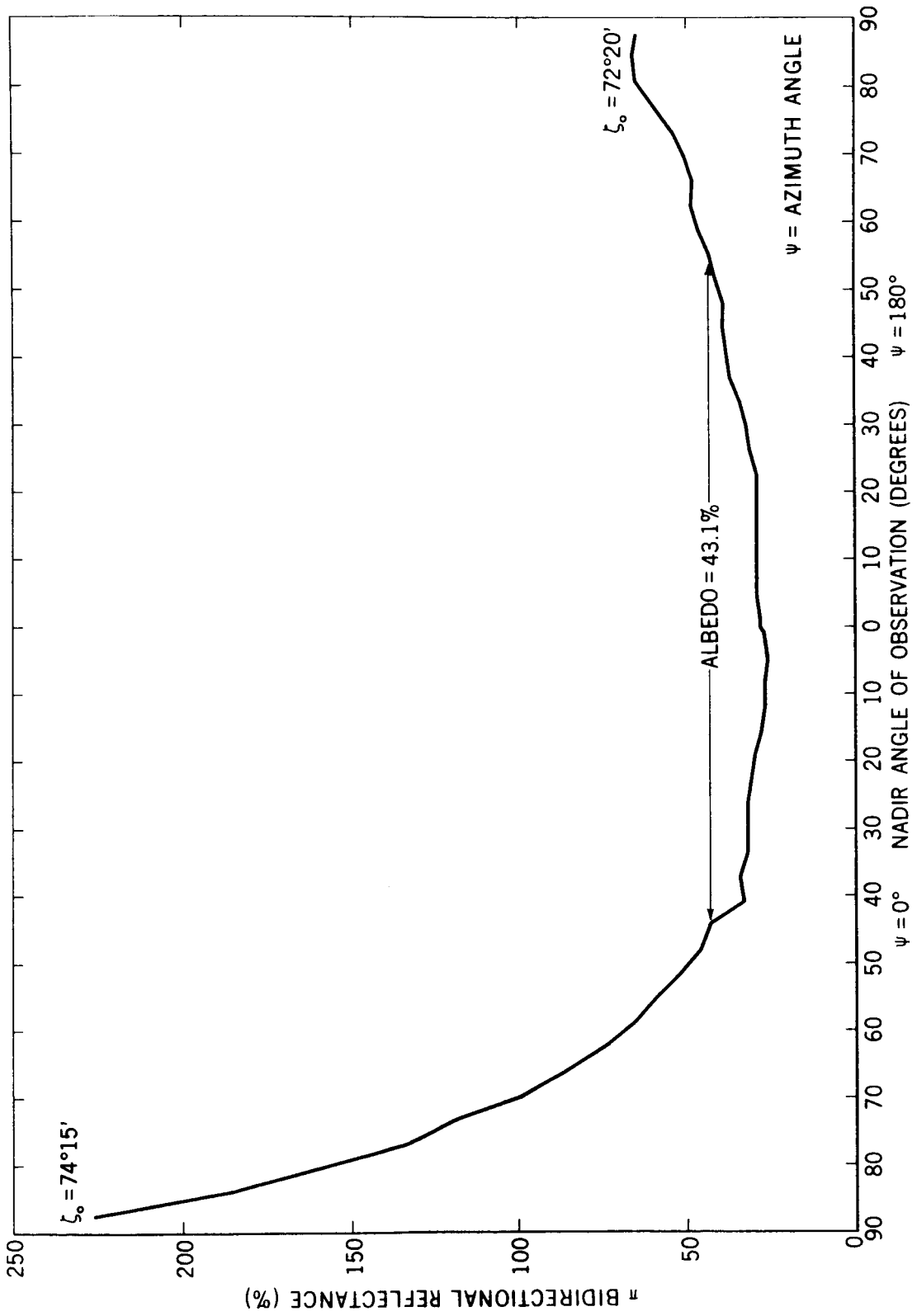


Figure 18—NASA Convair-990 Flight 36, June 15, 1966 (Alt. 40,000 Ft.) Overcast Stratocumulus (Alt. ~2,500 Ft.) 36.5°N., 125.0°W. (0111 U.T. to 0209 U.T.) MRIR Channel 5 (0.2 to 4 $\mu$ )

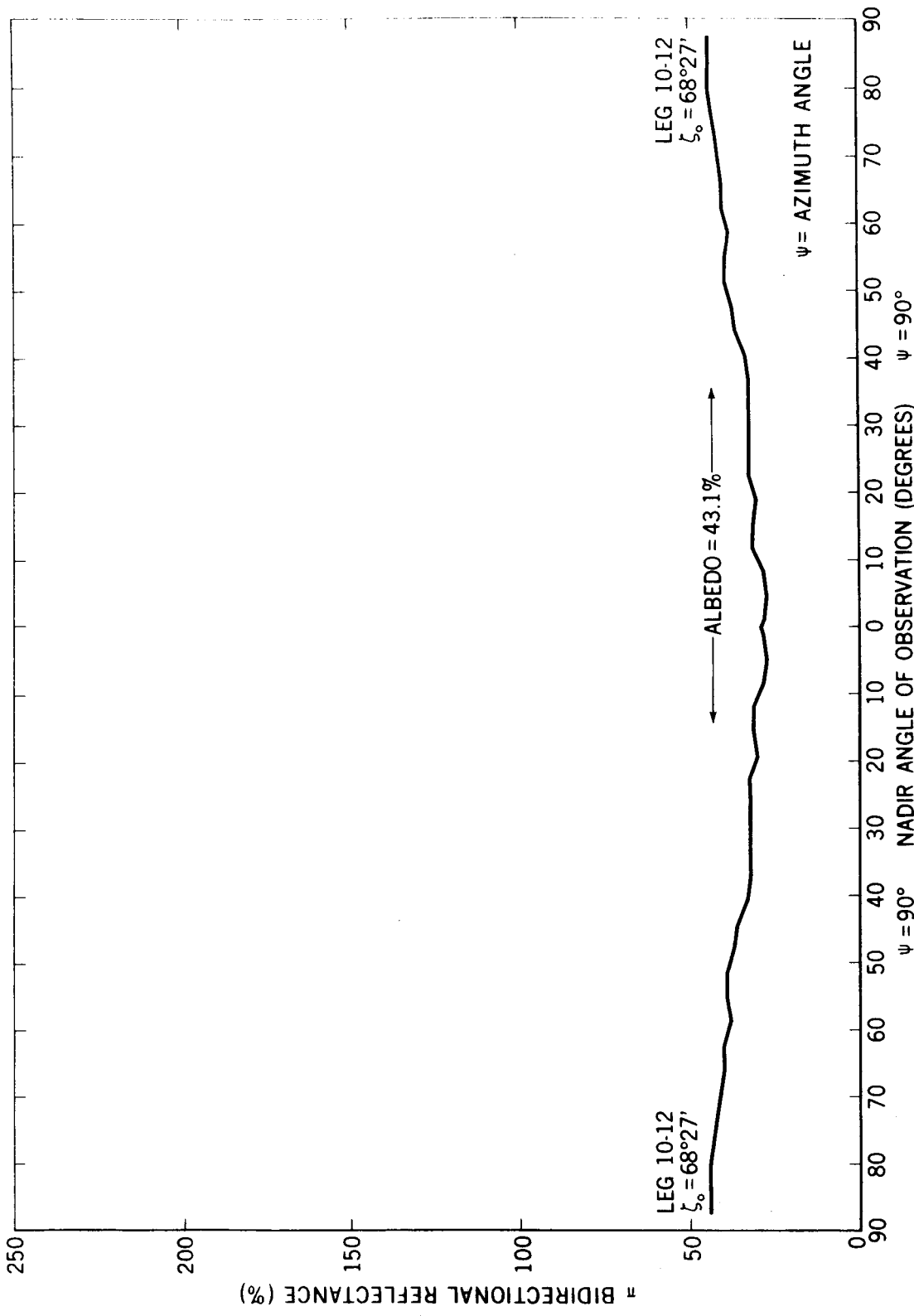


Figure 19—NASA Convair-990 Flight 36, June 14, 1966 (Alt. 40,000 Ft.) Overcast Stratocumulus (Alt. ~2,500 Ft.)  
 36.5°N., 125.0°W. (0111 U.T. to 0209 U.T.) MRIR Channel 5 (0.2 to 4 $\mu$ )

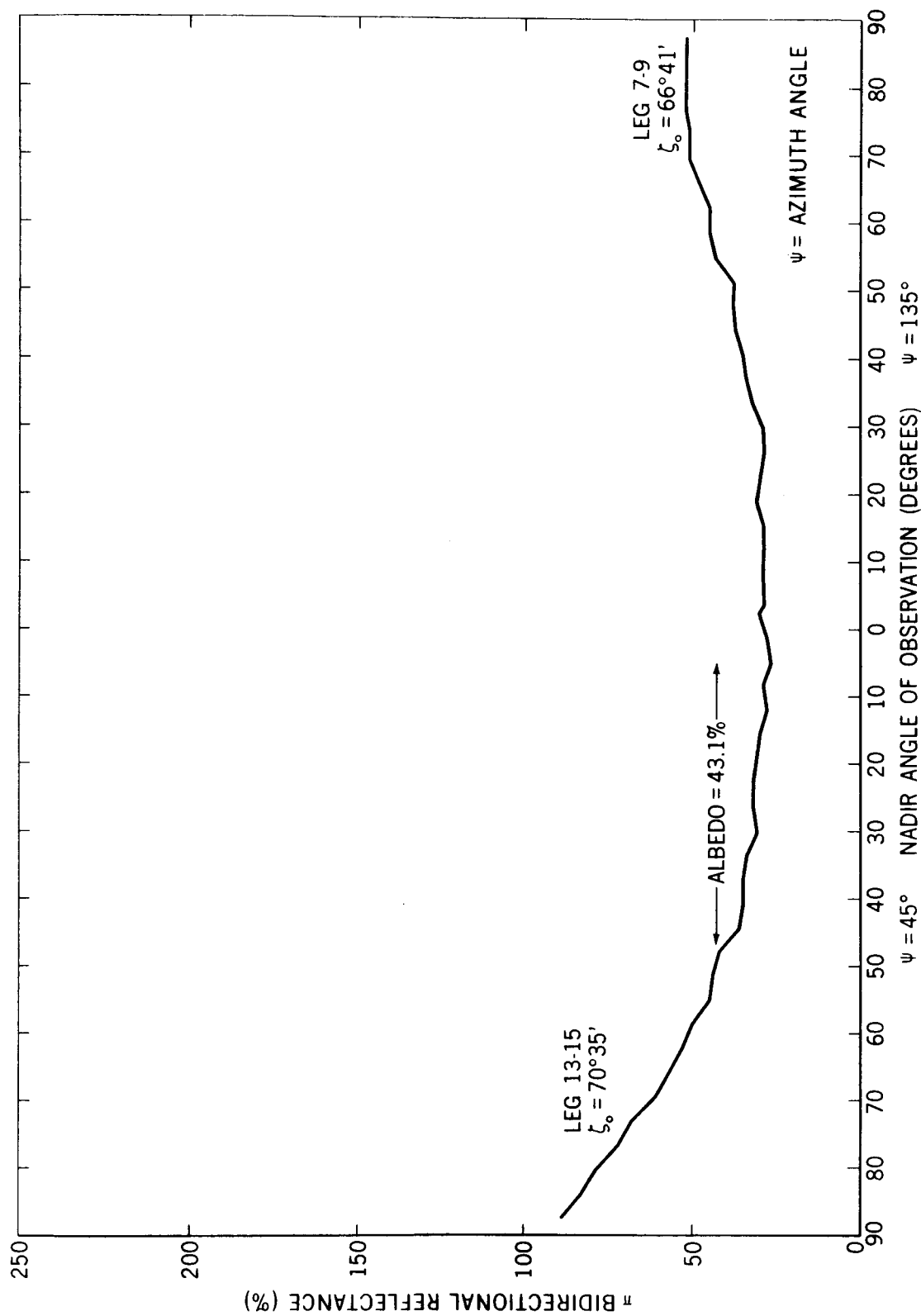


Figure 20—NASA Convair-990 Flight 36, June 14, 1966 (Alt. 40,000 Ft.) Overcast Stratocumulus (Alt. ~2,500 Ft.)  
 36.5° N., 125.0° W. (0111 U.T. to 0209 U.T.) MRIR Channel 5 (0.2 to 4μ)

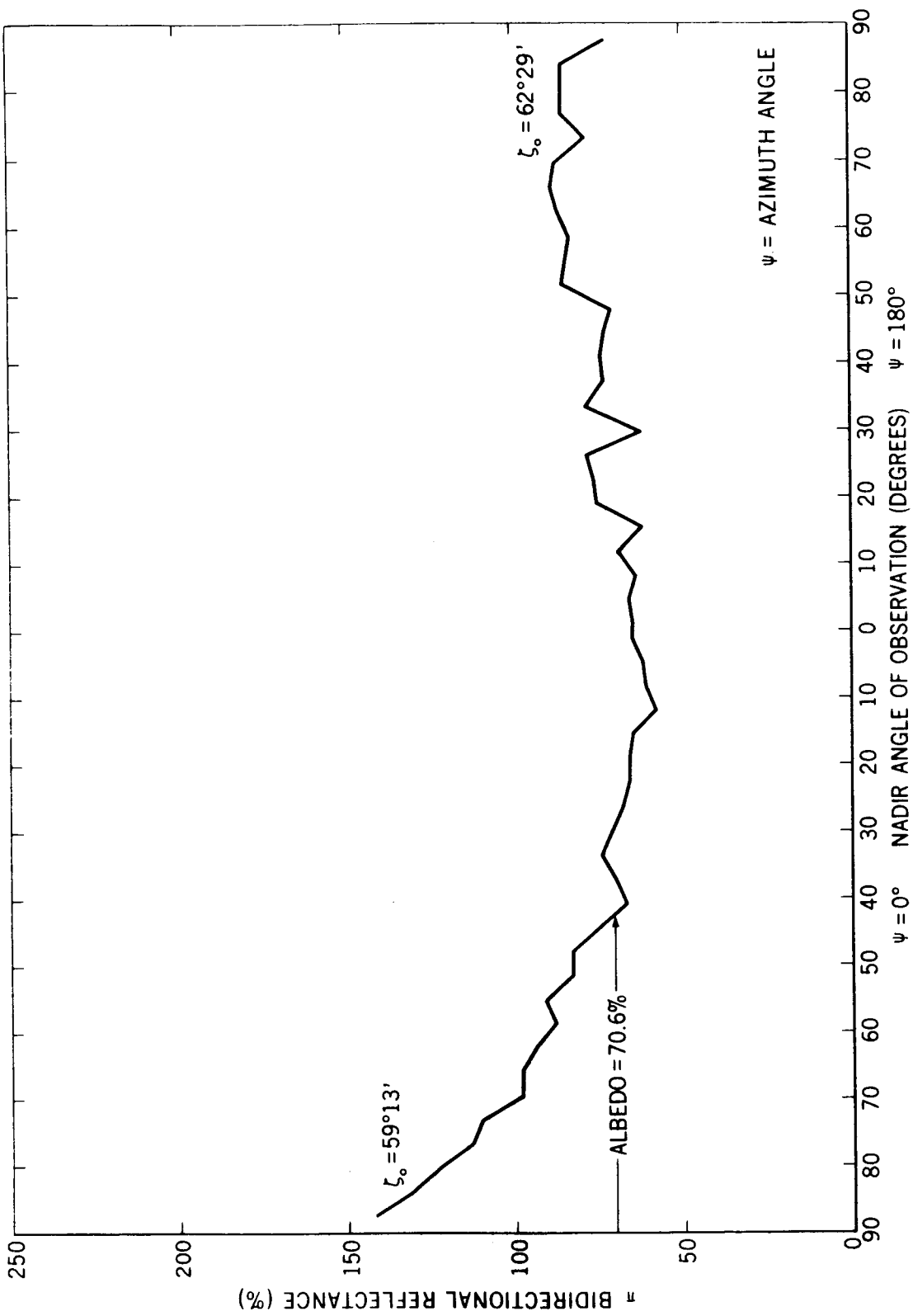


Figure 21—NASA Convair-990 Flight 14, May 11, 1966 Stratocumulus  $36^\circ 31'N.$ ,  $83^\circ 08'W.$  (21:45 U.T. to 22:52 U.T.)  
 MRIR Channel 3 (0.55 to  $0.85\mu$ )

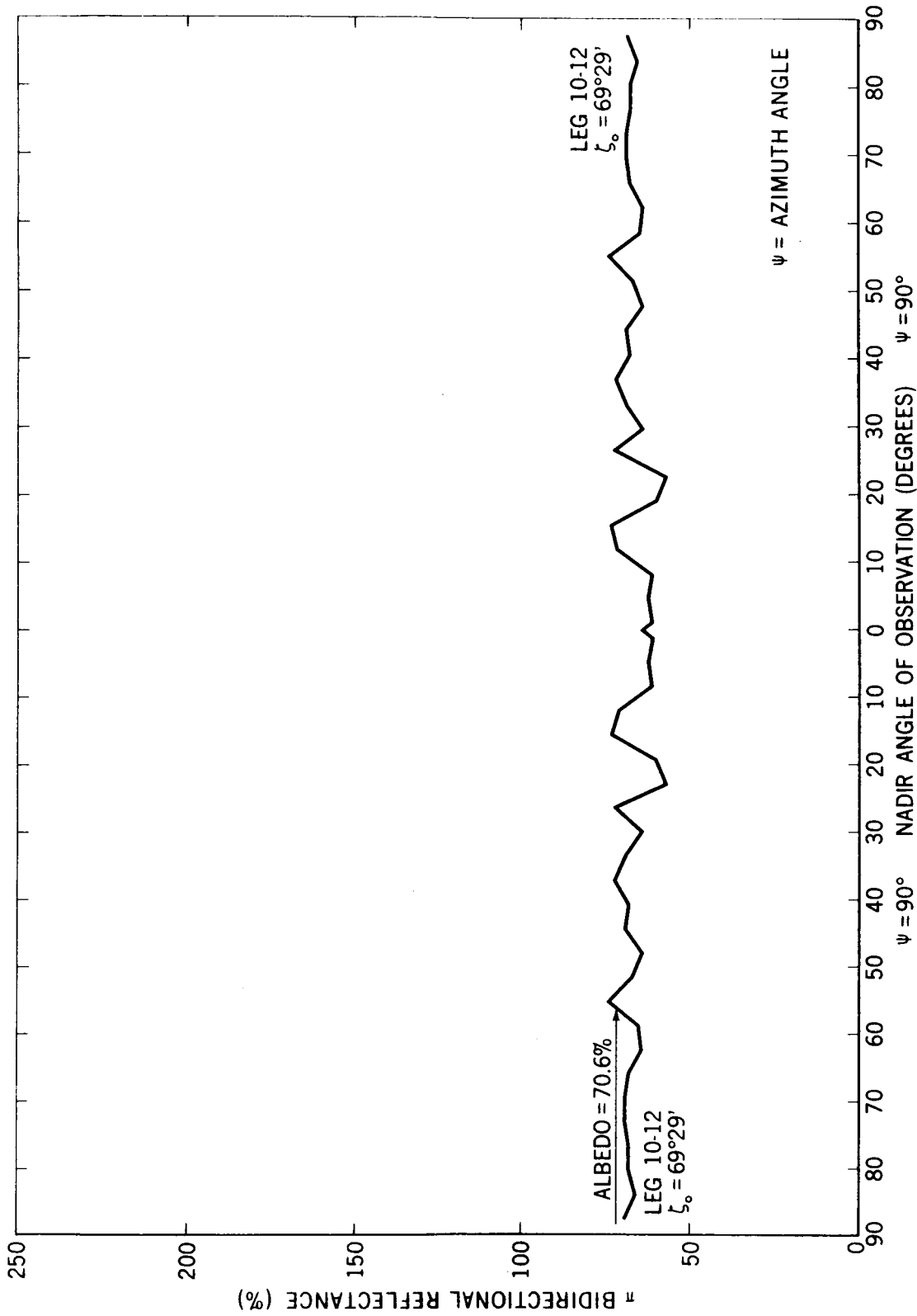


Figure 22--NASA Convair-990 Flight 14, May 11, 1966 Stratocumulus  $36^\circ 31'N$ ,  $83^\circ 08'W$ . (21:45 U.T. to 22:52 U.T.)  
 MIRIR Channel 3 (0.55 to  $0.85\mu$ )

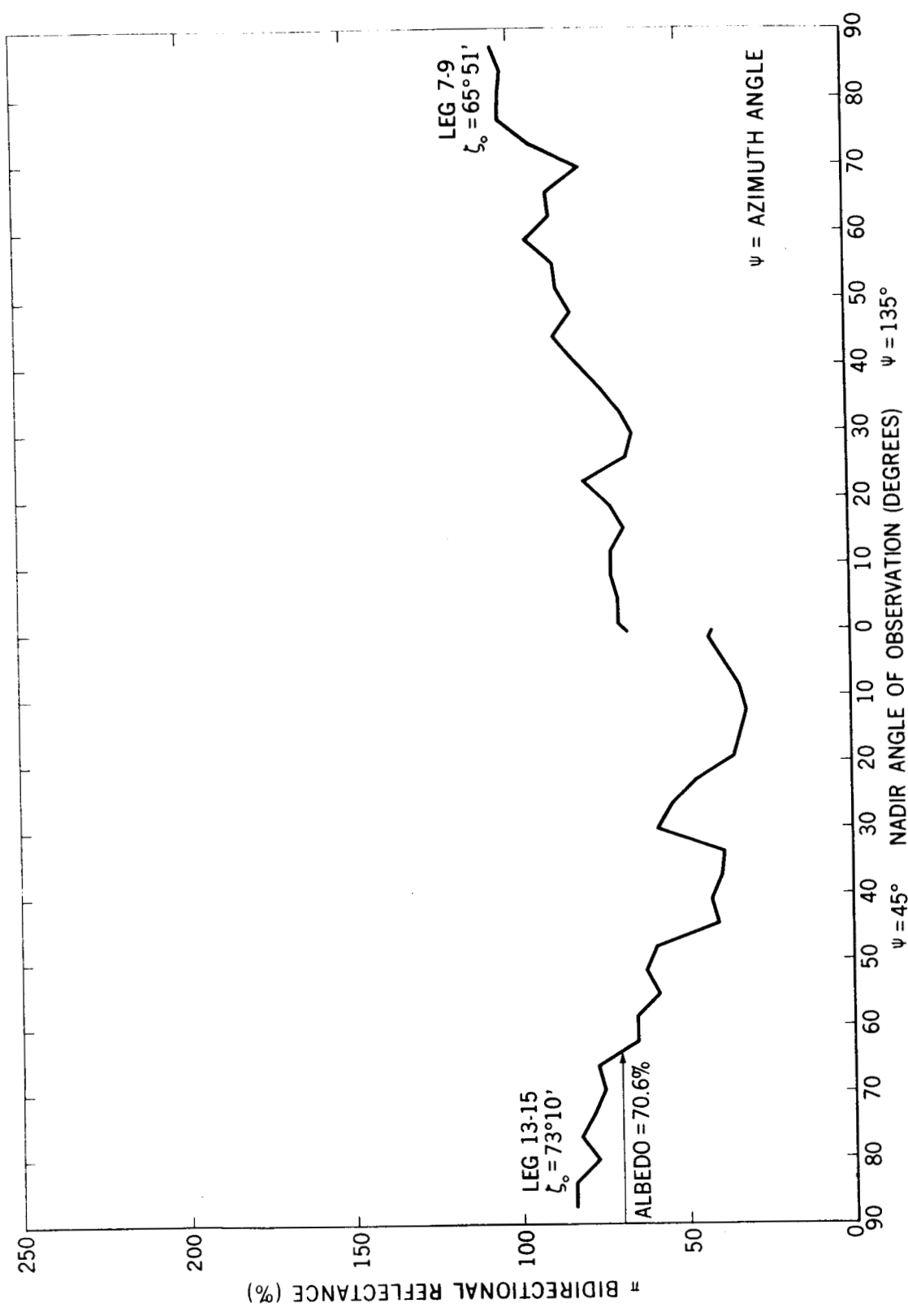


Figure 23—NASA Convair-990 Flight 14, May 11, 1966 Stratocumulus  $36^\circ 31'N$ ,  $83^\circ 08'W$ . (21:45 U.T. to 22:52 U.T.)  
 MRIR Channel 3 (0.55 to  $0.85\mu$ )

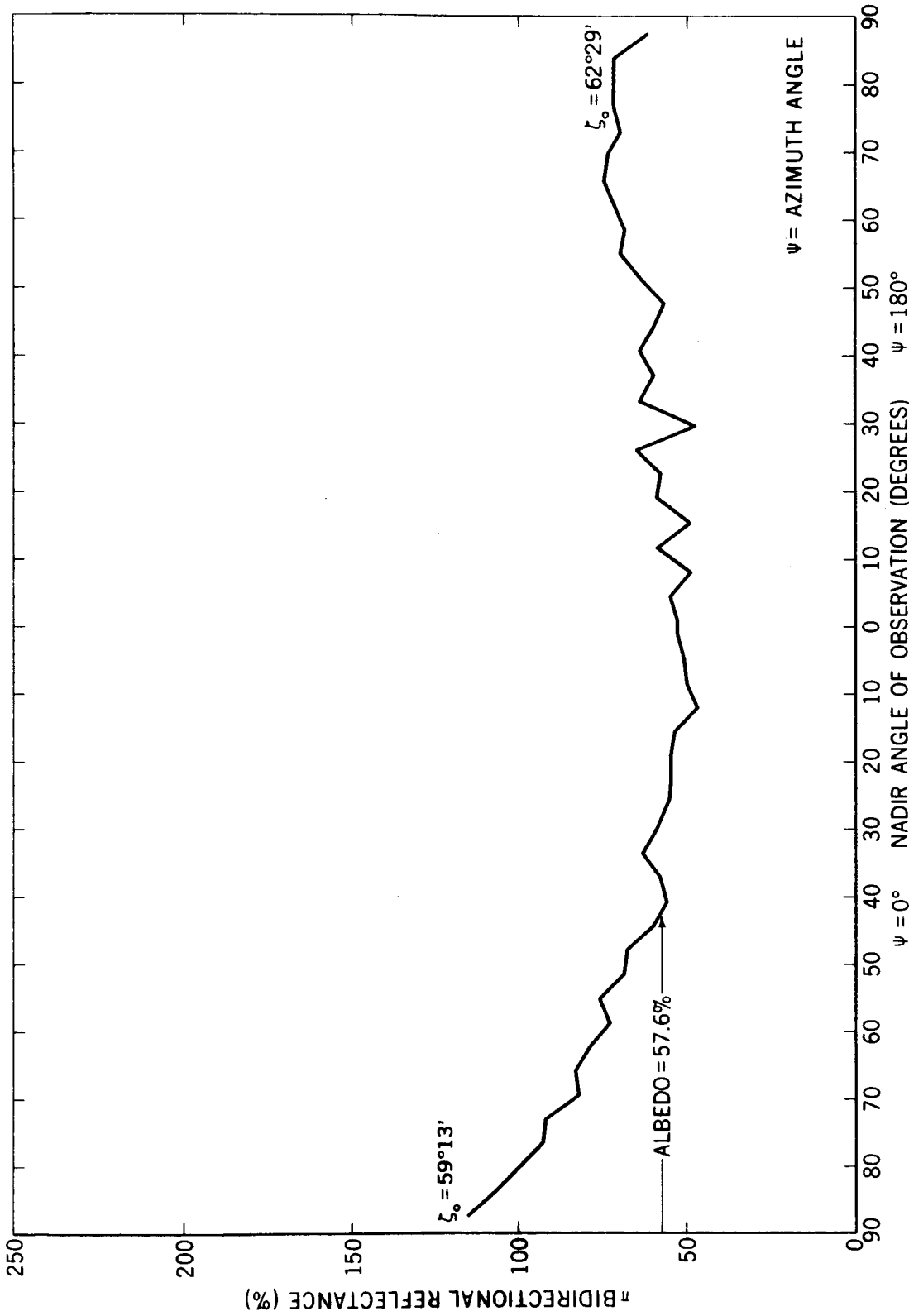


Figure 24—NASA Convair-990 Flight 14, May 11, 1966 Stratocumulus  $36^{\circ}31'N$ ,  $83^{\circ}08'W$ . (21:45 U.T. to 22:52 U.T.)  
 MRIR Channel 5 (0.2 to  $4\mu$ )

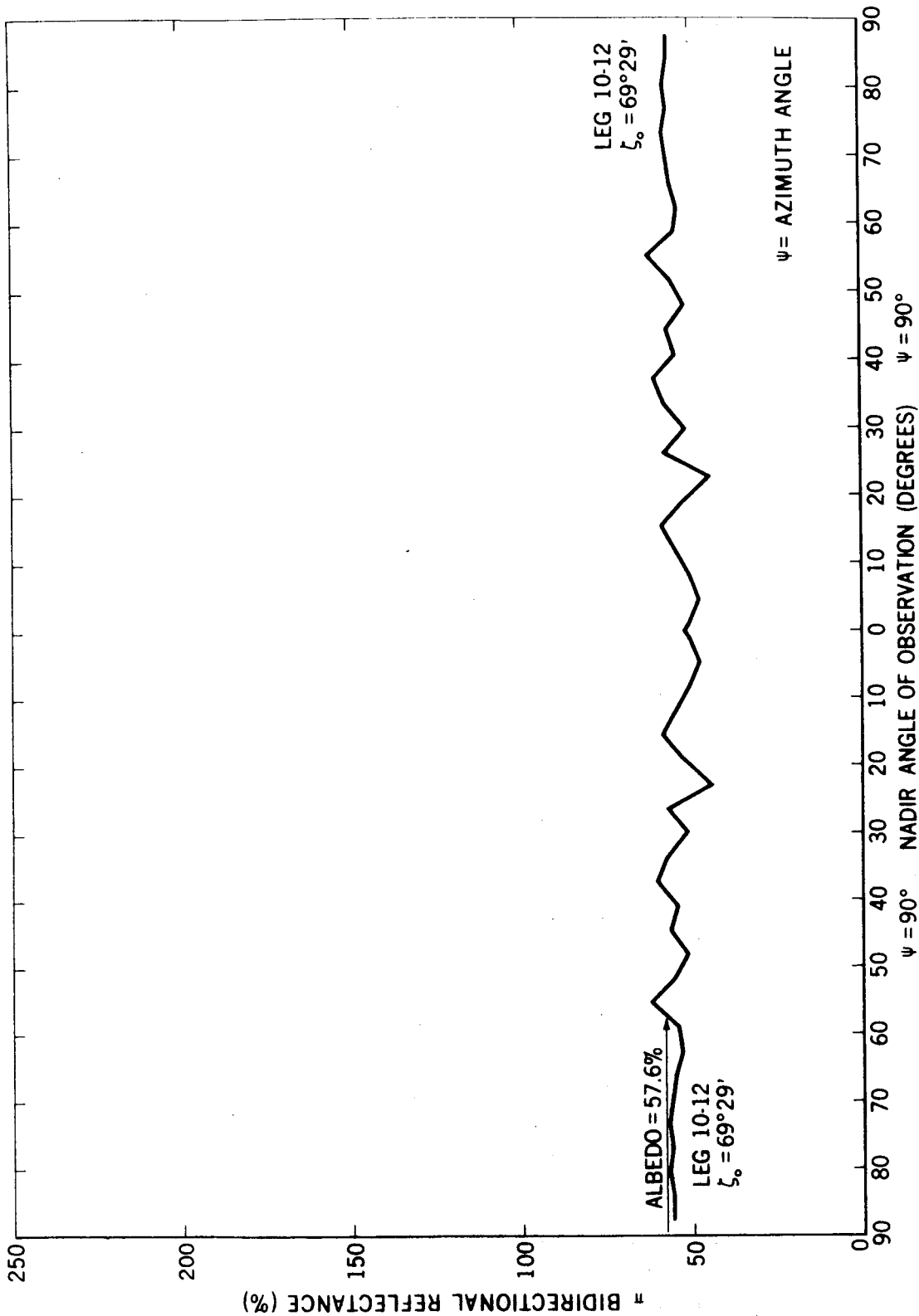


Figure 25—NASA Conveair-990 Flight 14, May 11, 1966 Stratocumulus  $36^\circ 31'N$ ,  $83^\circ 08'W$ . (21:45 U.T. to 22:52 U.T.)  
 MRIR Channel 5 (0.2 to  $4\mu$ )

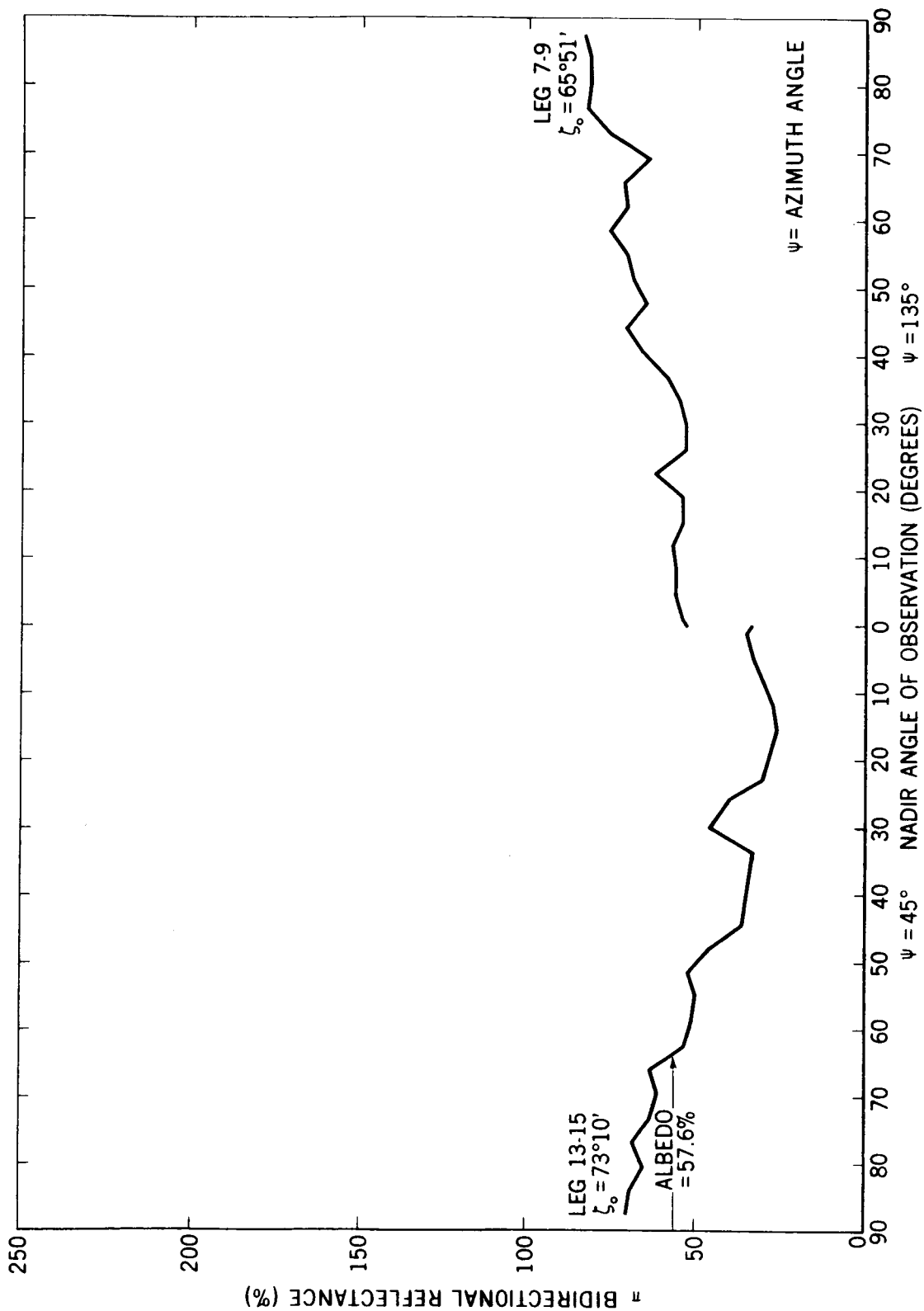


Figure 26--NASA Convair-990 Flight 14, May 11, 1966 Stratocumulus 36° 31' N., 83° 08' W. (21:45 U.T. to 22:52 U.T.)  
 MRIR Channel 5 (0.2 to 4 $\mu$ )